Clim. Past Discuss., doi:10.5194/cp-2015-186, 2016
Manuscript under review for journal Clim. Past
Published: 20 January 2016

Climate of the Past
Discussions
Open Access
EGU

Quantifying late-Holocene climate in the Ecuadorian Andes using a chironomid-based temperature inference model

Frazer Matthews-Bird[1&2], matthewsbirdf@fit.edu

Stephen J. Brooks[3], S.Brooks@nhm.ac.uk

Philip B. Holden[1], philip.holden@open.ac.uk

Encarni Montoya[1], encarni.montoya@open.ac.uk

William D. Gosling[1, 4], W.D.Gosling@uva.nl

[1]Department of Earth, Environment & Ecosystems, The Open University, Walton Hall, Milton Keynes, MK7 6AA, UK.

[2] Biological Sciences, Florida Institute of Technology, 150 West University Boulevard, Melbourne, FL 32901, USA

[3]Department of Life Sciences, Natural History Museum, Cromwell Road, London SW7 5BD, UK.

[4]Palaeoecology & Landscape Ecology, Institute for Biodiversity & Ecosystem Dynamics, University of Amsterdam, P.O. Box 94248, 1090 GE Amsterdam, The Netherlands

Corresponding author: Frazer Matthews-Bird

Key words: Bayesian, weighted-averaging, transfer function, chironomids, Holocene climate change, Ecuador

Clim. Past Discuss., doi:10.5194/cp-2015-186, 2016
Manuscript under review for journal Clim. Past
Published: 20 January 2016

Climate of the Past Discussions
Open Access
EGU

Abstract

Presented here is the first chironomid calibration dataset for tropical South America. Surface sediments were collected from 59 lakes across Bolivia (15 lakes), Peru (32 lakes) and Ecuador (12 lakes) between 2004 and 2013 over an altitudinal gradient from 150 m above sea level (a.s.l) to 4655 m a.s.l, between 0-17°S and 64-78°W. The study sites cover a mean annual temperature (MAT) gradient of 25°C. In total, 55 chironomid taxa were identified in the 59 calibration data-set lakes. When used as a single explanatory variable, MAT explains 12.9% of the variance (λ_1/λ_2= 1.431). Two inference models were developed using weighted averaging and Bayesian methods. The best performing model using conventional statistical methods was a WA (inverse) model (R^2_{jack}= 0.890, $RMSEP_{jack}$ = 2.404, Mean $bias_{jack}$= -0.017, Max bias $_{jack}$=4.665). The Bayesian method produced a model with R^2_{jack}= 0.909, $RMSEP_{jack}$ =2.373, Mean $bias_{jack}$= 0.598, Max bias $_{jack}$= 3.158. Both models were used to infer past temperatures from a *c.* 3000 yr record from the tropical Andes of Ecuador, Laguna Pindo. Inferred temperatures fluctuated around modern day conditions but showed significant departures at certain intervals (*c.* 1600 cal yr BP; *c.* 3000-2500 cal yr BP). Both methods (WA/Bayesian) showed similar patterns of temperature variability; however, the magnitude of fluctuations differed. In general the WA method was more variable often inferring unrealistically cold temperatures (*c.* -7±2.5°C relative to the modern). The Bayesian method provided temperature anomaly estimates for cool periods that lay within the expected range of the Holocene (*c.* -3±3.4°C). The chironomid-based MAT reconstruction from the Laguna Pindo fossil record suggests that periods of low solar output not only affect the tropics through changes in precipitation, but also directly affect tropical temperatures. Inferred temperatures were 2-3°C colder relative to the modern during the widely recognised 3500-2500 cal yr BP cooling event. Long-term cooling during the late-Holocene culminating in the Little Ice Age (LIA) is not apparent in the Laguna Pindo record. A cooling by 1-2°C relative to the modern during the LIA is recorded in a single fossil sample.

Clim. Past Discuss., doi:10.5194/cp-2015-186, 2016
Manuscript under review for journal Clim. Past
Published: 20 January 2016

Climate of the Past Discussions
Open Access
EGU

1. Introduction

Holocene climate variability (11.7 kcal yrs BP – present) offers the most recent opportunity to parameterise climate and ecosystem responses to natural forcing under current boundary conditions in the absence of intense anthropogenic activity (Mayewski *et al*., 2004; Oldfield and Steffen, 2014). Furthermore, quantitative estimates of past climate over long time scales (>1000 yrs) are vital to improving the reliability of modelling and prediction of present and future climate variability (Mayewski *et al*., 2004). The spatial distribution of palaeoclimate records, however, is currently uneven around the world. Quantitative reconstructions of past climate are common from mid- to high- latitudes of both hemispheres but data is much scarcer from low-latitude (tropical) regions (Jansen *et al.*, 2007). Tropical climate is the dominant driver of atmospheric circulation (Ivanochko *et al., 2005)* and the source of intermittent phenomena, such as the El Niño Southern Oscillation (ENSO), which has a global influence on climate (Collins *et al*., 2010). Quantitative estimates of past climate from the low latitude tropics, therefore, are crucial for investigating not only regional climate processes, but also teleconnections on long timescales (>1000 years) (Garreaud *et al.*, 2009; Jomelli *et al*., 2009; Vuille *et al*., 2000). Here we develop the first chironomid-based temperature inference model for tropical South America. The model is applied to a Holocene lake sediment sequence to generate the first quantitative chironomid-inferred temperatures from the tropical East Andean flank.

Chironomidae (non-biting midges) is a family of two-winged aquatic insects of the order Diptera. The family is globally distributed and one of the most diverse within aquatic ecosystems (Armitage *et al*., 1995). Many species are stenotopic, and their short life-cycles and ability to colonise favourable regions quickly means the insects are extremely sensitive to environmental change (Pinder, 1986). The head capsules of chironomid larvae are well preserved in lake sediments and have been used extensively as palaeoecological proxies (Brooks, 2006; Walker and Cwynar, 2006). Chironomid-based temperature inference models, derived from modern calibration data sets, have been applied across North America (reviewed in Walker and Cwynar, 2006), Eurasia (reviewed in Brooks, 2006), and more recently the method has been applied in the Southern Hemisphere in Patagonia (Massaferro and Larocque, 2013; Massaferro *et al*., 2014), Central America (Wu *et al*., 2014), East Africa (Eggermont *et al*., 2010), and Australasia (Dimitriadis and Cranston 2001; Woodward and Shurlmeister 2006).

Clim. Past Discuss., doi:10.5194/cp-2015-186, 2016
Manuscript under review for journal Clim. Past
Published: 20 January 2016

Transfer functions make a number of underlying assumptions; particularly the environmental variable to be reconstructed is an ecologically important determinant in the system, and environmental variables other than one being reconstructed have a negligible effect on species assemblages (Juggins, 2013). Rarely are ecological systems as simple as transfer functions would imply and violations of these assumptions will undermine the validity of the environmental reconstruction (Juggins, 2013). Nevertheless, despite known inherent problems associated with transfer functions (Huntley, 2012; Juggins, 2013; Velle *et al*., 2010), quantitative reconstructions from chironomid assemblages often produce consistent results that compare well with other proxy estimates of past temperature (Brooks, 2000; Brooks *et al.*, 2012; Heiri *et al*., 2007). The best performing inference models can reconstruct temperatures with errors of *c.* 1°C (Brooks and Birks, 2001; Eggermont et al., 2010; Heiri et al., 2003; Olander et al., 1999a; Rees et al., 2008; Self et al., 2011) providing high resolution insights into past changes in climate (Brooks and Langdon, 2014), and validation of climate models (Heiri *et al.*, 2014).

1.1 Holocene climate variability

Holocene climate variability is subdued (±2-3^{o}C) (Mayewski *et al*., 2004; O'Brien *et al.*, 1995) compared with the preceding Late Glacial period (*c.* 25,000-11,700 years before present [yrs BP], ±7-10^{o}C) (Alley, 2000; Anderson, 1997), nevertheless rapid climate change events are recognised in Holocene palaeoclimate records (Mayewski *et a*l., 2004). Changes in insolation caused by solar forcing is generally regarded as the dominant driver of global climate change during the Holocene (Mayewski *et al.*, 2004; Wanner *et al*., 2008). The Roman warm period (250 BC-400 AD [2200-1550 yrs BP]), and cooling during the Little Ice Age (LIA) (1350-1850 AD [600-100 yrs BP]) are well established features, notably across the Northern Hemisphere (Johnsen *et al*., 2001; O'Brien *et al*., 1995). Growing evidence from the tropics suggests Holocene climate fluctuations such as the LIA are probably global events (Thompson *et al*., 2002; Wanner *et al.*, 2008); however, additional quantitative palaeoclimate records are needed to understand the expression of such events in the tropics, and to clarify global climate teleconnections. Although the low latitudes receive 47% of planetary insolation, the climate response in the tropics to solar variability is poorly understood (Crowley, 2000; Polissar *et al.*, 2006).

Clim. Past Discuss., doi:10.5194/cp-2015-186, 2016
Manuscript under review for journal Clim. Past
Published: 20 January 2016

106 **1.2 Holocene climate variability in tropical South America**

107 The most notable feature of current South American climate is the annual migration of the Intertropical
108 Convergence Zone (ITCZ), which affects rainfall patterns across the tropical Andes (Abbott *et al.*, 2003; Bird *et*
109 *al.*, 2011; Haug *et al*., 2001). On Holocene timescales, however, there remain large uncertainties regarding the
110 patterns and processes of climate change in the Andes with evidence for both rapid (*c.* 100-1000 yr)
111 precipitation (Haug *et al*., 2001) and temperature variability (Thompson *et al*., 2006; Wanner *et al.*, 2008). A
112 further point to note is the spatial heterogeneity of Holocene climate variability in the tropical Andes (Baker and
113 Fritz, 2015a), particularly regarding precipitation. Ice core records from the Peruvian and Bolivian Andes since *c*.
114 5400 cal yrs BP suggest the overall trend is towards a drier climate with high amplitude fluctuations and periods
115 of significant aridity. Precipitation reached a minimum during the period between 3800-2800 cal yrs BP and the
116 LIA (Haug *et al*., 2001; Thompson *et al*., 1986; Thompson *et al*., 1995). Speleothem records from the Central
117 Andes of Peru contradict this, however, and indicate instead that from the 15th to 18th century precipitation was
118 on average about 10% higher than the present day (Reuter *et al*., 2009).

119 The mid- to late-Holocene (*c.* 6000 cal yrs BP to present) is a period of cooling climate in South America.
120 Pollen evidence suggests montane vegetation replaced Andean forest taxa as the treeline lowered with modern
121 vegetation patterns becoming established by *c.* 3000 cal yrs BP (Markgraf, 1989). Long-term cooling in the late
122 Holocene culminated in a minimum during the 17th and 18th centuries, coinciding with evidence for precipitation
123 minimum during the LIA in northern South America (Haug *et al*., 2001; Thompson *et al*., 1986; Thompson *et al*.,
124 1995). Further south, Patagonian proxy records infer periods that were wet and cold enough to allow glacial
125 advance (Meyer and Wagner, 2008).

126 Stable isotopic records derived from ice cores and speleothems provide some of the highest resolution
127 archives of South American palaeoclimate (Kanner *et al.*, 2013; Mosblech *et al*., 2012; Thompson *et al*., 1986;
128 Thompson *et al*., 1995). These records must be viewed cautiously, however, as the proxy also reflects a range of
129 environmental factors; changes in water vapour, snow surface histories, source and sink ratios, and the effect of
130 temperature on carbonate-water isotopic fractionation (Baker and Fritz, 2015; Leng and Marshall, 2004;
131 Thompson *et al*., 1986). Without solid constraints on temperature variability through time it is difficult to be
132 certain of the isotopic signal. In the South American tropics, where the relationship between changes in

Clim. Past Discuss., doi:10.5194/cp-2015-186, 2016
Manuscript under review for journal Clim. Past
Published: 20 January 2016

temperature and precipitation are complex (Baker *et al.*, 2001; Garreaud *et al.*, 2009), more independent quantitative estimates of past temperature are needed in order to resolve climate patterns over the tropical Andes during the Holocene.

1.3 Aims

In this study, we have developed the first chironomid-based temperature calibration data set from the tropical Andes (0 to 17°S). Surface sediment samples from 59 lakes along the eastern flank of the Andes to Amazonia are analysed. Two approaches are used to develop the inference model, the widely used weighted averaging method (Brooks and Birks, 2000) and a second using a Bayesian approach (Holden *et al.*, 2008) which has rarely been used before. The models are applied to fossil chironomid assemblages in a late-Holocene lake sediment record from Laguna Pindo, central Ecuador, to reconstruct mean annual temperature (MAT) changes over the past *c.* 3000 years.

2 Study Sites

2.1 Modern calibration dataset

Surface sediments were collected from 59 lakes across Bolivia (15 lakes), Peru (32 lakes) and Ecuador (12 lakes) between 2004 and 2013 over an altitudinal gradient from 150 m above sea level (a.s.l) to 4655 m a.s.l, between 0-17°S and 64-78°W (Fig 1). The study sites cover an MAT gradient of 25°C; the coldest lake in the data set is 0.8°C MAT and the warmest is 25°C MAT (Table 1). The deepest lake is 25 m and the shallowest is 0.1 m, mean water depth of all the study sites is 5 m. Cold, high elevation lakes are more common within the calibration data set and there are no lakes between 16°C and 20°C. Sediment samples used in this study were taken from the uppermost centimetre (0-1cm) which represents the most recent deposits (approx. 5-20 years) (Frey, 1988) and therefore most comparable with the available climate data for calibration.

Clim. Past Discuss., doi:10.5194/cp-2015-186, 2016
Manuscript under review for journal Clim. Past
Published: 20 January 2016

159 **2.2 Fossil chironomid record**

160 Laguna Pindo is a small shallow lake on the eastern flank of the Ecuadorian Andes (1°27.132'S;
161 78°04.847'W) (Fig1). The site is located at an elevation of 1248 m a.s.l. MAT is *c.* 20°C with little seasonal
162 variation and mean annual precipitation (MAP) can reach *c.* 4000 mm per year (Hijmans *et al*., 2005). Currently
163 the lake is not directly fed by a stream in-flow and has no visible stream out-flow; the lake receives water from
164 surface run-off and direct precipitation. There are no obvious geomorphological causes for the escarpment of
165 the lake and we hypothesise it is tectonic in origin.

166 At the time of field work (January 2013) maximum water depth was *c.* 1 m, the lake is heavily overgrown
167 with aquatic macrophytes making a detailed bathometric survey difficult. A sedimentary sequence 929 cm long
168 was extracted using a cam-modified piston Livingston corer (Colinvaux *et al*., 1999) from the centre of the lake
169 to minimise the chance of encountering a sedimentary gap caused by any periods of lake area reductions.
170 Sediments were recovered in aluminium tubes and sealed on site before being transported to the UK and
171 stored at *c.* 4°C. A total of 14 samples were analysed for ^{14}C radiocarbon using AMS dating at the SUERC
172 radiocarbon facility, East Kilbride. An age-depth model was created using version 2.2 of the statistical package
173 clam.R (Blaauw, 2010) and the Southern Hemisphere calibration curve SHCal13.14C (Hogg *et al.*, 2013).

174

175 **3. Methods**

176 **3.1 Chironomid analysis**

177 Chironomid preparation and identification from both lake surface and core sediments followed standard
178 methods as described by Brooks *et al* (2007). The wet sediment was deflocculated in 10% KOH for 2 minutes at
179 75°C. The sediment was then washed through 212µm and 90µm sieves with water. Chironomids were picked
180 from the residues in a Bogorov counting tray using a stereomicroscope at 25x magnification. Head capsules
181 were mounted in Euparal, ventral side up and identified to the highest possible taxonomic resolution under a
182 compound light microscope at 200-400x magnifications with reference to Wiederholm (1983), Epler (2001)
183 Rieradevall & Brooks (2001), Brooks *et al* (2007), Cranston (2010) and local taxonomic works including Prat *et al*
184 (2011), and Trivinho-Strixino (2011). Some taxa could not be formally identified and so were given informal
185 names. Images and descriptions of informally named taxa are provided in Matthews-Bird *et al* (2015).

Clim. Past Discuss., doi:10.5194/cp-2015-186, 2016
Manuscript under review for journal Clim. Past
Published: 20 January 2016

186

187 **3.2 Environmental variables**

188 Environmental variables (depth, pH, conductivity, and water temperature) were measured at each lake in
189 the field. Organic content of the sediment was established through Loss-on-ignition following standard methods
190 as described by Heiri et al (2001). Climate data (MAT, MAP) were obtained from high resolution, interpolated
191 climate surfaces (Hijmans *et al*., 2005). Elevation (m a.s.l.), latitude (decimal degrees), and longitude (decimal
192 degrees) were also included as variables in the calibration data set. A summary of all the environmental
193 variables measured can be found in Table 1.

194

195

196 **3.3 Exploratory statistics**

197 Detrended Correspondence Analysis (DCA) was initially used as an indirect ordination method to assess the
198 gradient lengths in compositional units of taxon turnover (Hill and Gauch, 1980). The gradient length of DCA axis
199 1 was 5.2 standard deviation units (SD), which suggests a unimodal response, and that linear ordination
200 methods were not appropriate (ter Braak, 1987). Canonical Correspondence Analysis (CCA) was used to explore
201 the influence of the measured environmental variables on the distribution and abundance of taxa. Highly
202 correlated variables were partialled-out by analysis of the variance of their regression coefficients indicated by
203 their Variance Inflator Factors (VIFs). Variables with high VIFs were systematically removed from the
204 environmental variable data set until the remaining variables had VIFs below 20. Detrended canonical
205 correspondence analysis (DCCA) was used to test how much of the variance in the assemblage data was
206 explained by each individual explanatory variable. The ratio of λ_1:λ_2 (i.e., the ratio of first constrained DCCA axis
207 1 and second unconstrained DCA axis 2) was used to assess the influence an explanatory variable has in
208 describing the variance in the chironomid community assemblage, and hence its predictive power (Juggins,
209 2013). All taxa were retained in the statistical analysis and rare taxa were down-weighted in the weighted
210 average transfer function (down-weighting of rare species is implicit in the Bayesian approach). Multivariate
211 analysis was carried out on square root transformed chironomid percentage data.

212

Clim. Past Discuss., doi:10.5194/cp-2015-186, 2016
Manuscript under review for journal Clim. Past
Published: 20 January 2016

213 **3.4 Inference models**

214 Inference models were developed using two separate approaches. The first method relied on weighted
215 averaging methods, a tried and tested technique well established in quantitative palaeoecology (Birks, 1998;
216 Birks *et al.*, 2012; ter Braak and Juggins, 1993; ter Braak and Looman, 1986). The second method uses a
217 Bayesian approach, which in general has received less attention (Holden *et al.*, 2008). There are a number of
218 inherent problems associated with quantitative inference models (Huntley, 2012; Juggins, 2013; Velle et al.,
219 2010) so the two independent methods were used to compare results and assess the strengths and weaknesses
220 of each method.

221

222 **3.5 Weighted averaging**

223 The assemblage data was unimodal suggesting transfer functions using weighted averaging partial least
224 squares (WA-PLS) were appropriate (ter Braak and Juggins, 1993). Inference models were also developed using
225 classical and inverse weighted averaging (WA) to compare performance. The optimal number of components
226 was assessed using leave-one-out cross validation (jack knifing) and a minimum 5% change in prediction error
227 between components. Sample specific errors for the inferred temperatures were obtained through
228 bootstrapping 999 cycles.

229

230 **3.6 Bayesian**

231 Bayesian model selection was used to generate probability-weighted species response curves (SRCs) for
232 each taxon in the calibration dataset. Each taxon is assigned 8,000 possible SRCs. Each of these SRCs has a
233 probability weight based on its relative ability to describe the training data for that taxon. To perform a
234 reconstruction, likelihood functions (temperature probability distributions) are derived from each taxon in a
235 fossil sample, considering all 8,000 SRCs. Combining the likelihood functions of all the taxa in the fossil sample
236 derives the reconstruction. The power of the Bayesian approach is that it ascribes a probability distribution to
237 the reconstruction, providing a reconstruction-specific uncertainty. An important benefit is that all taxa in the
238 sample provide potentially useful information, even those with low counts that would be largely neglected in a

Clim. Past Discuss., doi:10.5194/cp-2015-186, 2016
Manuscript under review for journal Clim. Past
Published: 20 January 2016

239 weighted averaging approach. To illustrate, a few counts of a taxon with a narrow temperature tolerance may
240 constrain the Bayesian reconstruction more than a very high count of a taxon with a broad tolerance.

241 Although the Bayesian model was developed for application to pH reconstructions from diatom
242 assemblages, it is generally applicable whenever it is appropriate to assume a unimodal species response to an
243 environmental gradient. The only modification required is the specification of appropriate priors. The *a priori*
244 probability distribution for optimum temperature in the SRCs was assigned to be uniform in the range -4.2 to
245 +30.8°C (training set range ±°5C). The *a priori* probability for SRC tolerance was assigned to be uniform in the
246 range 2 to 10°C. Other SRC priors were unchanged from those in Holden *et al*. (2008).

247

248 **3.7 Reliability of reconstructions**

249 DCCA detrending by segments, non-linear rescaling, and constrained by radiocarbon age was used to
250 determine compositional turnover constrained within the stratigraphic sequence (Birks and Birks, 2008). The
251 goodness-of-fit to temperature was evaluated by including the fossil chironomid samples passively in a CCA
252 ordination space of the modern training set samples constrained by MAT. Fossil samples with a squared residual
253 distance within the extreme 10% of the modern calibration dataset samples are considered as having a poor fit
254 to temperature. The modern analogue technique was used to test if fossil samples had good analogues within
255 the modern calibration data set. Any fossil sample with a squared chord distance larger than the 95% threshold
256 of the calibration data set is considered to have no good modern analogues (Birks, 1998; Velle *et al*., 2005).
257 Data were untransformed prior to analysing the dissimilarity using the modern analogue technique. The
258 significance of the final reconstruction was tested by comparing the amount of variance in the fossil data
259 explained by that reconstruction, compared with inferences produced by transfer functions trained on
260 randomly generated environmental data (Telford and Birks, 2011a). In this case, 999 random environmental
261 variables were generated in order to produce the null distribution.

262

263

264

Clim. Past Discuss., doi:10.5194/cp-2015-186, 2016
Manuscript under review for journal Clim. Past
Published: 20 January 2016

4. Results

4.1 Explanatory variables

The eight remaining explanatory variables, after those with VIFs >20 were removed; together explain 34.03% of the variance (Fig 2). The first two CCA axes explained 61.7% of the variance (λ_1=0.792, λ_2 = 0.466). MAT describes most of the variance in the chironomid assemblages and has the highest λ_1:λ_2 ratio (Table 2). When used as a single explanatory variable, MAT explains 12.93% of the variance (λ_1/λ_2= 1.431).

4.2 Calibration data set taxa

In total, 55 chironomid taxa were identified in the 59 training set lakes (Matthews-Bird et al., 2015). *Chironomus anthracinus*-type was the most widespread taxon, occurring over the entire temperature gradient (Fig 3). Orthocladiinae are generally most abundant towards the cold end of the temperature gradient (Matthews-Bird et al., 2015). *Cricotopus/Paratrichocladius* type III is the dominant taxon of the coldest lake and is not present in sites >10°C MAT. Figure 4 shows the weighted average and Bayesian optima and tolerance of each taxon ordered by lowest to highest optima as modelled in the weighted averaging approach. In general the temperature optima predicted by each method are similar, however, *Tanytarsus* type II and *Cricotopus/Paratrichocladius* type VII have colder optima when modelled using a Bayesian approach. *Cricotopus/Paratrichocladius* type IV has the coldest temperature optima *c.* 3.3°C (Fig 4). Few Chironominae were found at the cold end of the calibration data set, but, for example, *Parachironomus* and *Tanytarsus* type II were only found in lakes cooler than *c.* 8°C and had optima of *c.* 7.5°C and *c.* 6.5°C respectively. *Paratanytarsus* and *Pseudosmittia* are important components of the chironomid assemblage between 4-12°C, forming >50% of the chironomid community in some lakes, and have optima of *c.* 9.1 and 8.3°C respectively. *Tanytarsus* type I, *Micropsectra* and *Einfeldia* are dominant taxa at mid-temperatures between *c.* 10-22°C. The absence of lakes between *c.* 16°C and *c.* 20°C limits a complete understanding of the distribution of taxa occurring at these temperatures.

DCCA analysis, constrained by MAT, indicates an assemblage shift across the temperature gradient of 2.2 SD units. The biggest change in assemblage composition occurs above 12°C MAT (Fig 3). *Goeldichironomus*, *Cladotanytarsus* and *Tanytarsus* type III were only found in lakes with MAT warmer than *c.* 22°C. Tanypodinae

Clim. Past Discuss., doi:10.5194/cp-2015-186, 2016
Manuscript under review for journal Clim. Past
Published: 20 January 2016

were in greatest abundance at the warm end of the temperature gradient between *c.* 10-26°C, *Procladius* was the most common Tanypodinae. It occurred between *c.* 10-26°C and had an optimum of *c.* 21°C.

4.3 Inference models

Chironomid larval head capsule concentrations can vary significantly between lakes, due to differences in preservation or abundance. Low counts can have adverse effects on the performance of inference models and the reliability of quantitative environmental reconstructions when using conventional methods (Heiri and Lotter, 2001; Quinlan and Smol, 2001). A minimum count size of 50 head capsules per sample is advised (Heiri and Lotter, 2001; Quinlan and Smol, 2001), however, good model performance has been achieved even when several samples include as few as 15-30 head capsules (Massaferro *et al.*, 2014). In some lakes in the current training set head capsule concentrations were as low as two head capsules per gram of sediment. Fifteen lakes in the data set produced fewer than 50 head capsules, and three lakes had fewer than 30. On average 77 individuals were analysed from each lake with a minimum count of 23 and a maximum of 164 (Table 1). Lakes with low head capsule counts were retained in the model in order to maintain as even coverage as possible across the temperature gradient.

Both methods (WA and Bayesian) produced similar performance statistics. The best performing model using conventional statistical methods was a WA (inverse) model (Table 3, Fig 5)(R^2_{jack}= 0.890, $RMSEP_{jack}$ = 2.404, Mean $bias_{jack}$= -0.017, Max $bias_{jack}$=4.665). The Bayesian method produced a slightly higher performing model with R^2_{jack}= 0.909, $RMSEP_{jack}$ =2.373, Mean $bias_{jack}$= 0.598, Max $bias_{jack}$= 3.158.

4.4 Laguna Pindo fossil chironomids and dating

Chironomid remains were found only in the upper 416 cm of the 929cm sequence of Laguna Pindo (Fig 6). In total, 2489 individual chironomid head capsules were analysed. The entire assemblage was made up of 32 taxa in 26 genera and 4 subfamilies. Among the taxa identified, 17 were Chironomini, eight Orthocladiinae and three Tanypodinae. There was high variation between samples both in number of head capsules (average: 82; range: 24 - 184) and concentration per gram of wet sediment (average: 73; range: 2 - 163). There was a marked decline in head capsule concentration below 200 cm. In younger sediments (200-0 cm) head capsule

Clim. Past Discuss., doi:10.5194/cp-2015-186, 2016
Manuscript under review for journal Clim. Past
Published: 20 January 2016

concentration averaged 106/gram, in older samples (200-420 cm) the average was 44/gram. Five zones were identified using optimal partitioning with a broken stick model to define significant zones. *Polypedilum nubifer*-type, *Procladius* and *Limnophyes* were the most abundant taxa; abundances are over 10% wherever they occurred. *Tanytarsus* type II was most abundant below 200 cm (1500 cal yr BP) whilst *Polypedilum nubifer*-type was present in low numbers below 340 cm (2300 cal yr BP). During periods of low *Polypedilum nubifer*-type abundance, *Tanytarsus* type II and *Tanytarsus* type I occur in greater numbers (e.g. 420-360; 290-250 cm).

The best-fit age depth model for Laguna Pindo was a smooth spline (Fig S1). Due to the absence of chironomids at the bottom of the sequence, six radiocarbon samples were used for building the model with a total depth of the sediment considered of 461 cm (Table S1). The sedimentation rate ranged between 0.03 and 0.5 cm/yr, with a sampling interval resolution of 97 years between samples on average (range from 27 to 196 years).

4.5 Palaeotemperature reconstruction

Both transfer functions (WA inverse and Bayesian) show similar patterns in the temperature reconstruction (Fig 7). From 3000-2500 cal yr BP inferred temperatures are cold relative to the modern (20.2°C). The minimum WA inverse temperatures are much colder (13.5°C±2.5) than the inferred Bayesian temperatures (17.5°C±3.7) for the early section of the sequence. From 2400 to 1700 cal yr BP inferred temperatures from both methods oscillate around *c.* 18-19°C but remained depressed relative to the modern. A notable feature of both reconstructions is the sudden drop in inferred temperatures at 1600 cal yr BP. Inferred temperatures fall by *c.* 2°C to 17.5°C±2.7. This abrupt drop in temperature is short-lived in both reconstructions and temperatures return to previous values in the subsequent sample. From 1500 cal yr BP to the present the chironomid-inferred temperatures stabilise and steadily rise. Peak temperatures for the entire record (21.9°C±3.5) are inferred between 400-700 cal yr BP. Temperatures begin to cool from 400 cal yrs BP in both reconstructions, reaching a minimum of *c.* 17°C±2.5 *c.* 100 cal yr BP before rising rapidly to between 20-21°C±2.5 in the most recent sediment sample. On average the Bayesian model infers warmer temperatures than the WA model.

The fossil samples of Laguna Pindo plot within the modern variation of chironomid assemblages when included passively in a CCA analysis of the calibration data set (Fig 8). This suggests that the calibration dataset is appropriate for the fossil sequence of Laguna Pindo. The fossil samples plot along the MAP gradient

Clim. Past Discuss., doi:10.5194/cp-2015-186, 2016
Manuscript under review for journal Clim. Past
Published: 20 January 2016

345 suggesting precipitation is an important variable controlling the variance in the fossil assemblages. The sites
346 associated with high precipitation in the calibration dataset are located in the same region of the Ecuadorian
347 Andes as the fossil site. With a modern MAT of *c.* 20°C, Laguna Pindo is located in a region of the temperature
348 gradient that is poorly covered in the calibration dataset (Fig 3), although the samples plot within the range of
349 modern calibration lakes that lie at similar elevations (1000-3000 m a.s.l). Seven taxa found in the Laguna Pindo
350 sequence do not occur in any of the analysed calibration data set lakes. These include three unknown
351 morphotypes, three *Xestochironomus* morphotypes, and *Metriocnemus eurynotus*-type. These taxa, however,
352 never comprise more than 10% of the chironomid assemblage of any one sample.

353 Seven of the fossil samples are considered to have a poor goodness-of-fit to temperature and all fossil
354 samples are considered as having poor modern analogues in the calibration data set (Fig 9). Although the
355 modern analogue technique is not used to infer past temperatures the lack of modern analogues in the fossil
356 assemblage is important when considering the reliability of any reconstruction.

357 DCCA constrained by radiocarbon age shows an abrupt change at 1475 cal yr BP between zones 3 and 4
358 and a turnover of 1.6 SD units over the whole sequence (Fig 9). The most recent sample is clearly distinct from
359 any other period of the record. Much of the variation in goodness-of-fit and DCCA sample scores is mirrored by
360 changes in count size and head capsule concentration. The sudden drop in head capsule concentration occurs at
361 a step change in DCCA assemblage variation (1475 cal yrs BP) (Fig 9). Periods of increased count size and head
362 capsule concentration in older sediments (2100-2250 cal yrs BP) also coincides with periods of improved
363 goodness-of-fit (Fig 9). The WA classical inferred MAT values using the modern calibration data set explain more
364 of the variance than 95% of randomly generated variables and so the WA classical MAT reconstructions can be
365 deemed statistically significant (p= 0.032) (Fig 10) (Telford and Birks, 2011a).

366

367 **5. Discussion**

368 **5.1 Chironomids and environmental variables**

369 Chironomids have been shown to respond to temperature at a variety of spatial scales and taxonomic levels
370 (Brooks, 2006; Eggermont and Heiri, 2011). Temperature is a key variable in controlling chironomid
371 development at all stages of their life cycles, and influences voltinism, behaviour and metabolism (Armitage *et*

Clim. Past Discuss., doi:10.5194/cp-2015-186, 2016
Manuscript under review for journal Clim. Past
Published: 20 January 2016

372 *al*., 1995). Across the Northern Hemisphere, over large temperature gradients, mean July air temperature, the
373 warmest month of the year, which reflects the developmental period of most species, has been shown to be the
374 major determinant of variation in chironomid assemblages (Brooks, 2006; Walker and Cwynar, 2006). As a
375 result, many quantitative temperature inference models have been developed to reconstruct mean July air
376 temperature. Across the tropics however seasonal variation is small and many chironomids are multivoltine
377 (Walker and Mathews, 1987) so temperatures throughout the year are likely to be relatively more influential. In
378 tropical East Africa, Eggermont *et al*. (2010) demonstrated that mean annual air temperature was a significant
379 driver of chironomid assemblage composition and developed a chironomid-based inference model on this basis.
380 Similarly, Wu *et al*. (2014) showed MAT to be the most important environmental variable when developing a
381 chironomid inference model for Central America. When attempting to make quantitative inferences from fossil
382 assemblages it is first crucial to establish that the variable of interest is an important ecological determinant.
383 The variable to be reconstructed must describe a statistically important component of the variance within the
384 assemblage data (Juggins, 2013). Compared to other measured variables, mean annual temperature explained
385 the largest amount of chironomid assemblage variance and had the highest eigenvalue ratio (λ_1:λ_2) in the
386 Andean calibration dataset (Table 2). The explanatory strength of temperature in the calibration data set meets
387 the minimum criterion proposed by Juggins (2013) (i.e. λ_1:$\lambda_2 > 1.0$) for temperature being a suitable variable to
388 reconstruct from this calibration dataset.

389 The DCCA results suggest that precipitation is also a strong ecological determinant (λ_1:λ_2=0.9); the
390 passive plot of fossil samples with calibration samples further supports this conclusion. The fossil samples of
391 Laguna Pindo are strongly associated with MAP. Precipitation in Andean landscapes, however, is spatially
392 heterogeneous and geographically close localities experience significantly different rainfall patterns (Garreaud
393 *et al*., 2009). Lakes associated with high rainfall (Fig 2) are actually in areas of the northern Andes with two rainy
394 seasons a year. It is very likely that the bimodality of rainfall in these areas is as important in controlling
395 chironomid populations as the total amount of rainfall as measured by MAP. Precipitation is also intrinsically
396 linked to temperature as both temperature and precipitation increase with decreasing latitude in tropical South
397 America (Garreaud *et al*., 2009). Unlike temperature, precipitation affects chironomids indirectly making any
398 quantitative inference difficult. Precipitation will alter a suite of environmental variables (e.g. pH, conductivity,

Clim. Past Discuss., doi:10.5194/cp-2015-186, 2016
Manuscript under review for journal Clim. Past
Published: 20 January 2016

depth, substrate) making quantitative inferences of precipitation problematic. As chironomid life cycles are strongly controlled by temperature and many tropical chironomid species tend to be multivoltine, we suggest the most appropriate variable both ecologically and statistically to reconstruct using the Andean calibration data sets is MAT.

The optima and temperature tolerances (Fig 4) of many taxa found in the current study are similar to that noted in other Neotropical chironomid calibration datasets, further supporting the conclusion of temperature being an important ecological determinant. For example, Wu *et al*. (2014) in Central America, found taxa of the genera *Beardius*, *Labrundinia* and *Goeldichironomus* to have optima between 23-24°C whilst *Limnophyes* and *Corynoneura* where more abundant at the colder end of the gradient with optima of 15°C and 18°C respectively. In the current dataset *Beardius, Labrundinia*, and *Goeldichironomus* all have optima between 23-24°C and *Limnophyes* and taxa of *Corynoneura* also have optima of 15°C and 19°C, respectively. *Limnophyes* also has one of the broadest tolerances of all taxa in both calibration datasets suggesting the genus is probably represented by many species (Matthews-Bird et al., 2015). More work is needed in order to refine chironomid larval taxonomy in South America, however the current data suggest the potential for a larger calibration dataset applicable to wider area incorporating the Northern Neotropics and Central America.

5.2 Model performance

Although both models (WA inverse and Bayesian) perform well (WA RMSEP= 2.4°C and Bayesian RMSEP= 2.3°C), some of the best performing chironomid-based temperature inference models have prediction errors closer to 1.0°C (Brooks and Birks, 2001; Heiri *et al*., 2011, 2007; Olander *et al*., 1999). The highest performing chironomid inference models often have in excess of 100-150 calibration sites compared with just 59 in the current model and this may account for its reduced performance. Furthermore the lakes in the calibration data set are not evenly distributed over the temperature gradient. The cold end of the gradient has a higher number of lakes (34 cold, high elevation lakes) than at warm and intermediate temperatures (15 warm, mid-low elevation lakes). Uneven sampling has been shown to lead to biases which may reduce RMSEP (Telford and Birks, 2011b). Furthermore the over-representation of cold lakes in the current dataset may result in under-estimation of the temperature optima of some taxa and, therefore, bias temperature estimates towards cold

Clim. Past Discuss., doi:10.5194/cp-2015-186, 2016
Manuscript under review for journal Clim. Past
Published: 20 January 2016

426 values. In the Andean dataset, as analysis of residuals shows, temperatures around 10°C are often under-
427 estimated (Fig 5). Furthermore, the inferred temperatures of Laguna Pindo are on average cooler than the
428 modern day conditions.

429 The absence of lakes in part of the temperature gradient may limit the reliability of estimates of optima
430 and tolerances of taxa and also create 'edge effects' in the middle of the temperature range, in addition to
431 those that occur at the cold and warm end of the temperature gradient (Eggermont *et al*., 2010). Such problems
432 are inherent to WA models as predicted values are pulled towards the mean of the training set resulting in
433 under- and over-estimations of high and low values (ter Braak and Juggins 1993). However, despite having no
434 lakes between 16-20°C in the calibration data set, additional edge effects are not a feature of the current
435 inference model. The gap of c. 4°C does not appear to have compromised model performance, probably as the
436 interval is not significant and taxa have tolerances that span these temperatures.

437 *Polypedilum nubifer*-type and *Chironomus anthracinus*-type make up a large component of the
438 chironomid assemblages in lakes across the entire temperature gradient (Fig 3). Such eurythermic taxa probably
439 include several different species. It is difficult to model reliable, or even meaningful, optima for eurythermic
440 taxa. Poor model performance or unreliable reconstructions may result if the assemblage is dominated by
441 eurythermic taxa. We note that eurythermic taxa are described by high tolerance SRCs in the Bayesian
442 approach, leading to increased uncertainty in reconstructions through broad likelihood functions that
443 contribute little information to the posterior. Inferred temperature of *c.* 10°C, are likely to be underestimated as
444 many taxa found at these temperatures also occur in cold lakes, which are over-represented in the calibration
445 data-set. In African lakes Eggermont *et al*. (2010) found that the presence of eurythermic taxa such as
446 *Chironomus* type Kibos caused an overestimation of temperatures in lakes at the warm end of the gradient.
447 They also found that the occurrence of *Limnophyes minimus*-type and *Paraphaenocladius* type OI Bolossat
448 overestimated the temperature of lakes close to where gaps occurred in the gradient (Eggermont *et al*., 2010).
449 Similarly, in a New Zealand calibration data set developed by Woodward and Shulmeister (2006), *Chironomus*
450 was present in both high elevation, cold, oligotrophic lakes and lower elevation, warm, eutrophic lakes. The
451 intermediate temperature optimum estimated for this taxon resulted in over-estimated temperatures of cold
452 lakes and under-estimates of warm lakes (Woodward and Shulmeister, 2006). Eurythermic taxa may be

Clim. Past Discuss., doi:10.5194/cp-2015-186, 2016
Manuscript under review for journal Clim. Past
Published: 20 January 2016

453 contributing to the over-estimation of cold temperatures and the under-estimation of temperatures in the
454 middle of the gradient in the Andean inference model.
455
456 **5.3 WA vs Bayesian**
457 Despite similar performance statistics between the Bayesian and WA methods, the inferred pattern of late-
458 Holocene temperature change is different. Temperatures inferred c. 2700 cal yr BP (400 cm) (Fig 7) using the
459 WA inverse method is extremely cold (*c.* 14°C) compared with the rest of the record. This reconstruction is
460 driven by the high abundance of *Tanytarsus* type II, a taxon that has a WA temperature optimum of 6.5°C. The
461 Bayesian reconstruction for this sample of 17.8 ±2.8°C, is in line with more modest temperature shifts that
462 would be expected in the late-Holocene (Wanner *et al*., 2008). One advantage of the Bayesian methodology is
463 the transparency of the reconstruction through consideration of individual likelihood functions for this
464 assemblage (Fig 11). Although *Tanytarsus* type II is abundant in the sample its influence in the reconstruction is
465 moderated by several other taxa with higher temperature optima that are present at low abundances. This
466 temperature estimate demonstrates the Bayesian reconstruction can be sensitive to a few counts of a species
467 that have a negligible effect in a WA approach. The likelihood function for Chironomini type II, which has an
468 abundance of only 2.3% in the sample, constrains the reconstruction more than *Tanytarsus* type II, which has an
469 abundance of 74%. This is because Chironomini type II is only found in the warmest lakes in the calibration set, each
470 time with a low abundance. We note that because it is found in only three training set sites, Chironomini type II is
471 associated with many (671) high-probability SRCs, defined as having a probability great that 10% of the most likely
472 SRC. For this reason, its likelihood function is relatively broad and extends to temperatures far lower than the
473 temperature of the sites in which the taxon is found in the training set.
474
475 **5.4 Laguna Pindo temperature reconstruction**
476 It is important that the study site is appropriate for the calibration data set. The variable of interest must be
477 the most important in driving biotic change (Velle *et al*., 2005) especially considering the influence of important
478 secondary variables. It would be difficult to generate statistically significant reconstructions from fossil
479 assemblages that are influenced by several variables acting together (Telford and Birks, 2011a). Laguna Pindo is

Clim. Past Discuss., doi:10.5194/cp-2015-186, 2016
Manuscript under review for journal Clim. Past
Published: 20 January 2016

located at 1248 m a.s.l on the eastern Andean flank at the transition between the cold environments of the high Andes and warmer lowlands of the Amazon basin. Therefore, cold climatic periods during the lake's history would promote the migration of cold stenothermal taxa from higher elevations down the Andean flank to occupy the lake (Čiamporová-Zaťovičová *et al*., 2010). Conversely, during warm periods, taxa inhabiting lowland lakes would move up the Andean flank. Despite the influence of precipitation the location of Laguna Pindo makes it a good palaeoecological setting to record the response of temperature-sensitive proxies.

5.5 Temperature and secondary environmental variables

Whilst the λ1/λ2 of 1.431 indicates that MAT is appropriate for reconstruction using this calibration dataset (Juggins, 2013), it does not necessarily mean that reliable temperature reconstructions can be obtained from a fossil record (Telford and Birks, 2011a). Before attempting to interpret any reconstruction several metrics can be used to assess the validity of a reconstruction (Juggins and Telford, 2012).

The modern analogue technique compares the similarity of the fossil samples to the modern samples in the calibration data set. All fossil samples are greater than the 5th percentile of the square chord distance (Fig 9), which suggests there is no close modern analogue in the calibration set to any fossil sample (Birks, 1998; Juggins and Birks, 2001). The lack of modern analogues in the Laguna Pindo fossil sequence is due to the many taxa present in the fossil samples that are not present in the calibration data set. This may reflect the lack of lakes in the calibration dataset with MAT values close to those of Laguna Pindo. Nevertheless, WA and WAPLS models have been shown to perform well in non-analogue situations (Birks *et al*., 2010). The Bayesian method generates temperature reconstructions from likelihood functions of species in the calibration data set. Although analogous assemblages are not required for the Bayesian reconstruction (each taxon is treated equally and individually), species that are absent from the training set cannot contribute information to the posterior, thereby increasing the uncertainty associated with the reconstruction. One advantage of the Bayesian methodology is that this uncertainty is explicitly incorporated into the Bayesian reconstruction (Holden *et al*., 2008).

During periods of poor fit-to-temperature, variables other than temperature may have been affecting the composition of the chironomid assemblage. As noted previously, the CCA biplot of fossil samples included

Clim. Past Discuss., doi:10.5194/cp-2015-186, 2016
Manuscript under review for journal Clim. Past
Published: 20 January 2016

507 passively with the significant explanatory variables (Fig 8) shows that MAP was also important in driving the
508 assemblage variance. During times of poor fit to temperature the influence of precipitation as a secondary
509 variable may be more important than temperature in influencing the chironomid assemblage composition.
510 Indeed, precipitation has been shown to be an important variable in controlling the modern distribution of
511 chironomid taxa in the tropical Andes (Matthews-Bird et al., 2015).

512 Samples with poor fit-to-temperature also corresponded with samples having low numbers of head
513 capsules. The number of head capsules retrieved will directly affect how representative a sample is to the
514 chironomid fauna (Heiri, 2004; Quinlan and Smol, 2001). The cold oscillations inferred from the Bayesian
515 reconstruction are more in line with what is expected during the late-Holocene (1-3°C); the likelihood functions
516 of rare species which favour warm conditions combine to rule out the anomalously cold temperatures
517 suggested by some of the WA reconstructions. As discussed above, the over-representation of cold lakes in the
518 calibration dataset will likely bias species optima to colder values in a weighted average approach so there may
519 be a tendency for the model to underestimate temperature, especially during cold periods. This problem is
520 likely exaggerated when head capsule concentration is low, cold indicator taxa may have higher abundances
521 than would be the case if all taxa were accurately represented.

522 The DCCA results indicate that there was a distinct change in the composition of the chironomid
523 assemblage after 1600 cal yr BP (210 cm). This largely coincides with an increase in head capsule concentration,
524 possibly indicating an increase in lake productivity, and the shift in chironomid-inferred temperatures from low
525 to high. Indeed post 1600 cal yr BP, (210 cm) samples are inferred as being on average 2-3°C warmer than early
526 sections using Bayesian and WA models respectively.

527 Although the temperature reconstruction has a good ecological basis, because chironomids globally are
528 highly sensitive to temperature and Laguna Pindo is on an ecotonal boundary that is sensitive to temperature
529 changes, precipitation is influential as a secondary variable. The WA inverse MAT reconstruction, however, is
530 statistically significant based on the criteria described by Telford and Birks (2011a) (Fig 10) suggesting that
531 despite conflicting variables a temperature signal can be obtained from Neotropical chironomids.

532

Clim. Past Discuss., doi:10.5194/cp-2015-186, 2016
Manuscript under review for journal Clim. Past
Published: 20 January 2016

533 **5.6 Cooling climate 3800-2800 cal yrs BP**

534 Changes in insolation are often inferred as the dominant driver of Holocene climate changes (Mayewski *et*
535 *al.*, 2004). The period between 3500-2500 cal yr BP is recognised globally as a period of rapid climate change,
536 with changes in precipitation and temperature recorded globally from a range of different proxies (Mayewski *et*
537 *al.*, 2004; van Geel *et al.*, 1999). The most notable feature of South American Holocene climate is the migration
538 of the ITCZ, which affects rainfall patterns and is caused by changes in insolation affecting tropical Pacific sea
539 surface temperatures (Bird *et al.*, 2011; Haug *et al.*, 2001). The period between 3800-2800 cal yrs BP is a time of
540 erratic rainfall in the Caricao Basin of Venezuela, which resulted in pronounced aridity (Haug *et al.*, 2001) and
541 coincides with a maximum in $\Delta^{14}C$ and ^{10}Be, indicating a decline in solar output (Mayewski *et al.*, 2004). The low
542 chironomid-inferred temperatures between 3000-2500 cal yr BP probably reflect this decline in solar output
543 allowing high Andean taxa to migrate down slope. Our data suggests reduced insolation, as well as changing
544 precipitation patterns, could have the effect of cooling tropical climate.
545
546 **5.7 Recent cooling**
547 Prominent among climate fluctuations of the last millennium is the Little Ice Age (LIA), an event recognised
548 globally from historical and proxy climate records (Jones and Mann, 2004; Mayewski *et al.*, 2004). The peak and
549 duration of the LIA varies around the globe. In the tropical Andes a cold period, identified as the LIA, has been
550 recorded as early as 1180 AD (770 cal yr BP) and lasting as late as 1820 AD (130 cal yr BP) based on evidence of
551 glacial advance in mountain glaciers (Polissar *et al.,* 2006). The extent of LIA fluctuations remain unclear in the
552 tropics due to the paucity of quantitative palaeoclimate data (Crowley, 2000). Variation in the sun's energy
553 output is regarded as the main driver of LIA cooling. Although the tropics receive 47% of planetary insolation,
554 the climate response in the tropics to solar variability is poorly understood (Crowley, 2000; Polissar *et al.*, 2006).
555 The chironomid-inferred temperatures from Laguna Pindo suggest cooler temperatures from 400 cal yrs BP (50
556 cm) (1550 AD), reaching a minimum *c.* 100 cal yrs BP (20cm)(1850 AD), before rising again to the present day.
557 The inferred temperature minimum for this period is 17.7 ± 3.8°C which suggests a cooling of 2.2°C relative to
558 the modern temperature. We caution this estimate is within the RMSEP of the inference model and only
559 recorded in a single sample making any interpretations tentative. Multiple lines of evidence, however, do

Clim. Past Discuss., doi:10.5194/cp-2015-186, 2016
Manuscript under review for journal Clim. Past
Published: 20 January 2016

support a cooling in the tropical Andes similar in magnitude to that inferred here. Glacier fluctuations indicate a cooler and wetter climate than today for the outer and inner tropics of South America between the 17th and 19th century (Jomelli *et al.*, 2009). The Huascaràn and Quelccaya ice core records (Thompson *et al.*, 1986; Thompson *et al.*, 1995) from Peru suggest the latter half of the Holocene was a period of long-term cooling, reaching a minimum during the LIA, synchronous with Northern Hemisphere cooling. Temperature estimates from stable isotope data are difficult to generate, however, as the proxy is affected by changes in snow surface histories (Thompson *et al.*, 1986; Thompson *et al.*, 1995). Polissar *et al* (2006), using pollen and evidence of glacial retreat from the Venezuelan Andes, estimated a mean annual temperature reduction of 3.2±1.4°C relative to modern averages during the LIA. The chironomid-inferred temperatures at Laguna Pindo do not show the late-Holocene cooling trend culminating in the LIA, as recorded in the Andean ice core records. Instead temperatures remain relatively stable from 1500 cal yrs BP (195 cm), with a peak for the entire 3000 year record c. 400 cal yrs BP (50 cm) (21.8°C), followed by a drop in temperatures of 3-4°C beginning around 200 cal yrs BP (30 cm). This fluctuation is similar in magnitude to other records from the tropical Andes (Polissar *et al.*, 2006) however a higher resolution dataset is needed to investigate this trend further.

6. Conclusions

The chironomid fauna of the tropical Andes have been shown to be sensitive to climate variables, particularly temperature and precipitation. Both variables (MAT and MAP) meet the basic criteria for being used in an environmental reconstruction using the Andean calibration dataset. MAT, however, is an important determinant of chironomid species distribution and abundance and was therefore more appropriate to be reconstructed. The influence of precipitation should be explored further and must be considered as an important secondary variable especially when reconstructing past conditions in the region. It is very likely that the influence of precipitation noted here relates to the annual variability in rainfall across the Andes as opposed to overall amount making any quantitative interpretations even more difficult.

The two techniques used to develop inference models (WA and Bayesian) show comparable performance statistics (WA inverse model R^2_{jack}= 0.890, $RMSEP_{jack}$ = 2.404, Mean $bias_{jack}$= -0.017, Max $bias_{jack}$=4.665; Bayesian model R^2_{jack}= 0.909, $RMSEP_{jack}$ =2.373, Mean $bias_{jack}$= 0.598, Max $bias_{jack}$= 3.158). This work demonstrates a

586 proof of method, however, a larger calibration dataset with a more even coverage of calibration sites is needed
587 in order to improve model performance. The Bayesian approach provided a transparent reconstruction less
588 susceptible to the effect of an uneven distribution of calibration sites and performed particularly well during
589 periods of low count size and when inferring cold intervals. The chironomid-based MAT reconstruction from the
590 Laguna Pindo fossil record suggests that periods of low solar output not only affect the tropics through changes
591 in precipitation, but also directly affect tropical temperatures. Inferred temperatures were 2-3°C cooler relative
592 to the modern during the widely recognised 3500-2500 cal yr BP cooling event. Long-term cooling during the
593 late Holocene is not apparent in the Laguna Pindo record. However, temperatures do cool by 1-2.2°C relative to
594 the modern during the LIA period, although this is only noted in a single fossil sample.

595 Knowledge of past tropical climate dynamics is fundamental not only to understanding regional climate
596 but also global climate patterns and hemispherical teleconnections. Quantitative temperature proxies, such as
597 chironomids, will provide valuable data on past climate variability in the region. The reconstructions presented
598 here demonstrate the potential of the proxy and also highlights the complexity of late-Holocene climate change
599 in tropical South America.

600

601

602 **Acknowledgements**

603 Funding was provided by the Natural Environment Research Council (NERC), UK. NERC grant (ref:
604 NE/J018562/1) was awarded to E. Montoya and (ref: NE/J500288/1) awarded to F. Matthews-Bird. This work
605 was supported by the NERC Radiocarbon Facility NRCF010001 (allocation number 1682.1112) Special thanks to
606 Dr Pauline Gulliver for her continuous involvement and support during radiocarbon dating. The authors also
607 wish to thank Mark Bush, Francis Mayle, Yarrow Axford, Alex Chepstow-Lusty and Mick Frogley for their kind
608 donation of samples.

609

610

Clim. Past Discuss., doi:10.5194/cp-2015-186, 2016
Manuscript under review for journal Clim. Past
Published: 20 January 2016

References

Abbott, M.B., Wolfe, B.B., Wolfe, A.P., Seltzer, G.O., Aravena, R., Mark, B.G., Polissar, P.J., Rodbell, D.T., Rowe, H.D., Vuille, M., 2003. Holocene paleohydrology and glacial history of the central Andes using multiproxy lake sediment studies. Palaeogeogr. Palaeoclimatol. Palaeoecol. 194, 123–138. doi:10.1016/S0031-0182(03)00274-8

Alley, R.B., 2000. The Younger Dryas cold interval as viewed from central Greenland. Quat. Sci. Rev. 19, 213–226.

Anderson, E.D., 1997. Younger Dryas research and its implications for understanding abrupt climatic change. Prog. Phys. Geogr. 21, 230–249.

Armitage, P.D., Cranston, P.S., Pinder, L.C.V., 1995. The Chironomidae: the biology and ecology of nonbiting midges. London: Chapman and Hall.

Baker, P. a., Fritz, S.C., 2015a. Nature and causes of Quaternary climate variation of tropical South America. Quat. Sci. Rev. 124, 31–47. doi:10.1016/j.quascirev.2015.06.011

Baker, P. a., Fritz, S.C., 2015b. Nature and causes of Quaternary climate variation of tropical South America. Quat. Sci. Rev. 124, 31–47. doi:10.1016/j.quascirev.2015.06.011

Baker, P.A., Seltzer, G.O., Fritz, S.C., Dunbar, R.B., Grove, M.J., Tapia, P.M., Cross, S.L., Rowe, H.D., Broda, J.P., 2001. The history of South American tropical precipitation for the past 25,000 years. Science 291, 640–643. doi:10.1126/science.291.5504.640

Bird, B.W., Abbott, M.B., Vuille, M., Rodbell, D.T., Stansell, N.D., Rosenmeier, M.F., 2011. A 2,300-year-long annually resolved record of the South American summer monsoon from the Peruvian Andes. Proc. Natl. Acad. Sci. U. S. A. 108, 8583–8. doi:10.1073/pnas.1003719108

Birks, H.J.B., 1998. Numerical tools in palaeolimnology–Progress, potentialities and problems. J. Paleolimnol. 20, 307–332.

Birks, H.J.B., Birks, H.H., 2008. Biological responses to rapid climate change at the Younger Dryas--Holocene transition at Krakenes, western Norway. The Holocene 18, 19–30. doi:10.1177/0959683607085572

Birks, H.J.B., Heiri, O., Seppä, H., Bjune, A.E., 2010. Strengths and Weaknesses of Quantitative Climate Reconstructions Based on Late-Quaternary Biological Proxies. Open Ecol. J. 3, 68–110.

Birks, H.J.B., Lotter, A.F., Juggins, S., Smol, J.P. (Eds.), 2012. Tracking Environmental Change Using Lake Sediments; Data Handling and Numerical Techniques. Springer Netherlands.

Blaauw, M., 2010. Methods and code for “classical” age-modelling of radiocarbon sequences. Quat. Geochronol. 5, 512–518. doi:10.1016/j.quageo.2010.01.002

Brooks, S.J., 2006. Fossil midges (Diptera: Chironomidae) as palaeoclimatic indicators for the Eurasian region. Quat. Sci. Rev. 25, 1894–1910. doi:10.1016/j.quascirev.2005.03.021

Brooks, S.J., 2000. Chironomid-inferred Late-glacial air temperatures at Whitrig Bog, Southeast Scotland. J. Quat. Sci. 15, 759–764.

646 Brooks, S.J., Axford, Y., Heiri, O., Langdon, P.G., Larocque-Tobler, I., 2012. Chironomids can be reliable proxies
647 for Holocene temperatures. A comment on Velle et al. (2010). The Holocene 22, 1495–1500.
648 doi:10.1177/0959683612449757

649 Brooks, S.J., Birks, H.J.B., 2001. Chironomid-inferred air temperatures from Lateglacial and Holocene sites in
650 north-west Europe: progress and problems. Quat. Sci. Rev. 20, 1723–1741. doi:10.1016/S0277-
651 3791(01)00038-5

652 Brooks, S.J., Birks, H.J.B., 2000. Chironomid-inferred late-glacial and early-Holocene mean July air temperatures
653 for Kråkenes Lake, western Norway. J. Paleolimnol. 23, 77–89.

654 Brooks, S.J., Langdon, P.G., 2014. Summer temperature gradients in northwest Europe during the Lateglacial to
655 early Holocene transition (15–8 ka BP) inferred from chironomid assemblages. Quat. Int. 1–11.
656 doi:10.1016/j.quaint.2014.01.034

657 Brooks, S.J., Langdon, P.G., Heiri, O., 2007. The Identification and use of Palaearctic Chironomidae Larvae in
658 Palaeoecology. QRA Technical Guide No. 10, Quaternary Research Association, London.

659 Čiamporová-Zaťovičová, Z., Hamerlík, L., Šporka, F., Bitušík, P., 2010. Littoral benthic macroinvertebrates of
660 alpine lakes (Tatra Mts) along an altitudinal gradient: a basis for climate change assessment. Hydrobiologia
661 648, 19–34. doi:10.1007/s10750-010-0139-5

662 Colinvaux, P., De Oliveira, P.E., Patino, J.E.., 1999. Amazon Pollen Manual and Atlas. Harwood Academic
663 Publishers.

664 Collins, M., An, S.-I., Cai, W., Ganachaud, A., Guilyardi, E., Jin, F.-F., Jochum, M., Lengaigne, M., Power, S.,
665 Timmermann, A., Vecchi, G., Wittenberg, A., 2010. The impact of global warming on the tropical Pacific
666 Ocean and El Niño. Nat. Geosci. 3, 391–397. doi:10.1038/ngeo868

667 Cranston, P.S., 2010. No Title [WWW Document]. URL http://chirokey.skullisland.info/.

668 Crowley, T.J., 2000. Causes of Climate Change Over the Past 1000 Years. Science (80-.). 289, 270–277.
669 doi:10.1126/science.289.5477.270

670 Dimitriadis, S., Cranston, P.S., 2001. An Australian Holocene climate reconstruction using Chironomidae from a
671 tropical volcanic maar lake. Palaeogeogr. Palaeoclimatol. Palaeoecol. 176, 109–131.

672 Eggermont, H., Heiri, O., 2011. The chironomid-temperature relationship: expression in nature and
673 palaeoenvironmental implications. Biol. Rev. Camb. Philos. Soc. 87, 430–456. doi:10.1111/j.1469-
674 185X.2011.00206.x

675 Eggermont, H., Heiri, O., Russell, J., Vuille, M., Audenaert, L., Verschuren, D., 2010. Paleotemperature
676 reconstruction in tropical Africa using fossil Chironomidae (Insecta: Diptera). J. Paleolimnol. 43, 413–435.
677 doi:10.1007/s10933-009-9339-2

678 Epler, J.H., 2001. Identification manual for the Larval Chironomidae (Diptera) of South Carolina.

679 Frey, D.G., 1988. Littoral and offshore communities of diatoms, cladocerans and dipterous larvae, and their
680 interpretation in paleolimnology. J. Paleolimnol. 179–191.

681 Garreaud, R.D., Vuille, M., Compagnucci, R., Marengo, J., 2009. Present-day South American climate.
682 Palaeogeogr. Palaeoclimatol. Palaeoecol. 281, 180–195. doi:10.1016/j.palaeo.2007.10.032

683 Haug, G.H., Hughen, K.A., Sigman, D.M., Peterson, L.C., Röhl, U., 2001. Southward migration of the intertropical
684 convergence zone through the Holocene. Science 293, 1304–8. doi:10.1126/science.1059725

685 Heiri, O., 2004. Within-lake variability of subfossil chironomid assemblages in shallow Norwegian lakes. J.
686 Paleolimnol. 32, 67–84. doi:10.1023/B:JOPL.0000025289.30038.e9

687 Heiri, O., Brooks, S.J., Birks, H.J.B., Lotter, A.F., 2011. A 274-lake calibration data-set and inference model for
688 chironomid-based summer air temperature reconstruction in Europe. Quat. Sci. Rev. 30, 3445–3456.
689 doi:10.1016/j.quascirev.2011.09.006

690 Heiri, O., Brooks, S.J., Renssen, H., Bedford, A., Hazekamp, M., Ilyashuk, B., Jeffers, E.S., Lang, B., Kirilova, E.,
691 Kuiper, S., Millet, L., Samartin, S., Toth, M., Verbruggen, F., Watson, J.E., van Asch, N., Lammertsma, E.,
692 Amon, L., Birks, H.H., Birks, H.J.B., Mortensen, M.F., Hoek, W.Z., Magyari, E., Muñoz Sobrino, C., Seppä, H.,
693 Tinner, W., Tonkov, S., Veski, S., Lotter, A.F., 2014. Validation of climate model-inferred regional
694 temperature change for late-glacial Europe. Nat. Commun. 5, 4914. doi:10.1038/ncomms5914

695 Heiri, O., Cremer, H., Engels, S., Hoek, W.Z., Peeters, W., Lotter, A.F., 2007. Lateglacial summer temperatures in
696 the Northwest European lowlands: a chironomid record from Hijkermeer, the Netherlands. Quat. Sci. Rev.
697 26, 2420–2437. doi:10.1016/j.quascirev.2007.06.017

698 Heiri, O., Lotter, A., 2001. Effect of low count sums on quantitative environmental reconstructions: an example
699 using subfossil chironomids. J. Paleolimnol. 26, 343–350.

700 Heiri, O., Lotter, A.F., Hausmann, S., Kienast, F., 2003. A chironomid-based Holocene summer air temperature
701 reconstruction from the Swiss Alps. The Holocene 13, 477–484.

702 Heiri, O., Lotter, A.F., Lemeke, G., 2001. Loss on ignition as a method for estimating organic and carbonate
703 content in sediments: reproducibility and comparability of results. J. Paleolimnol. 25, 101–110.

704 Hijmans, R.J., Cameron, S.E., Parra, J.L., Jones, P.G., Jarvis, A., 2005. Very high resolution interpolated climate
705 surfaces for global land areas. Int. J. Climatol. 25, 1965–1978. doi:10.1002/joc.1276

706 Hill, M., Gauch, H.., 1980. Detrended correspondence analysis: an improved ordination technique. Vegetatio 42,
707 47–58.

708 Hogg, A.G., Hua, Q., Blackwell, P.G., Niu, M., Buck, C.E., Guilderson, T.P., Heaton, T.J., Palmer, J.G., Reimer, P.J.,
709 Reimer, R.W., Turney, C.S.M., Zimmerman, S.R.H., 2013. SHCal13 Southern Hemisphere calibration, 0–
710 50,000 cal yr BP. Radiocarbon 55, 1889–1903.

711 Holden, P.B., Mackay, A.W., Simpson, G.L., 2008. A Bayesian palaeoenvironmental transfer function model for
712 acidified lakes. J. Paleolimnol. 39, 551–566. doi:10.1007/s10933-007-9129-7

713 Huntley, B., 2012. Reconstructing palaeoclimates from biological proxies: Some often overlooked sources of
714 uncertainty. Quat. Sci. Rev. 31, 1–16. doi:10.1016/j.quascirev.2011.11.006

715 Ivanochko, T., Ganeshram, R., Brummer, G., Ganssen, G., Jung, S., Moreton, S., Kroon, D., 2005. Variations in
716 tropical convection as an amplifier of global climate change at the millennial scale. Earth Planet. Sci. Lett.
717 235, 302–314. doi:10.1016/j.epsl.2005.04.002

718 Jansen, E., Overpeck, J., Briffa, K.., Duplessy, J.-C., Joos, F., Masson-Delmotte, V., Olago, D., Otto-Bliesner, B.,
719 Peltier, W.., Rahmstorf, S., Ramesh, R., Raynaud, D., Rind, O., Solomina, O., Villalba, R., Zhang, D., 2007.
720 Climate Change 2007: The Physical Science Basis. Contribution of Working Group I to the Fourth
721 Assessment Report of the Intergovvernmental Panel on Climate Change, in: Solomon, S., Qin, D., Manning,

M., Chen, Z., Marquis, M., Averyt, K.B., Tignor, M., Miller, H.. (Eds.), . Cambridge University Press, Cambridge, United Kingdom and New York, NY, USA.

Johnsen, S.J., Dahl-Jensen, D., Gundestrup, N., Steffensen, J.P., Clausen, H.B., Miller, H., Masson-Delmotte, V., Sveinbjornsdottir, A.E., White, J., 2001. Oxygen isotope and palaeotemperature records from six Greenland ice-core stations: Camp Century, Dye-3, GRIP, GISP2, Renland and NorthGRIP. J. Quat. Sci. 16, 299–307. doi:10.1002/jqs.622

Jomelli, V., Favier, V., Rabatel, A., Brunstein, D., Hoffmann, G., Francou, B., 2009. Fluctuations of glaciers in the tropical Andes over the last millennium and palaeoclimatic implications: A review. Palaeogeogr. Palaeoclimatol. Palaeoecol. 281, 269–282. doi:10.1016/j.palaeo.2008.10.033

Jones, P., Mann, M., 2004. Climate over past millennia. Rev. Geophys. 42, 1–42. doi:10.1029/2003RG000143.CONTENTS

Juggins, S., 2013. Quantitative reconstructions in palaeolimnology: new paradigm or sick science? Quat. Sci. Rev. 64, 20–32. doi:10.1016/j.quascirev.2012.12.014

Juggins, S., Birks, H.J.B., 2001. Quantitative Environmental Reconstructions from Biological Data, in: Birks, H.J.B., Lotter, A.F., Juggins, S., Smol, J.P. (Eds.), Tracking Environmental Change Using Lake Sediments, Developments in Paleoenvironmental Research 5. pp. 431–494.

Juggins, S., Telford, R.J., 2012. Exploratory Data Analysis and Data Display, in: Birks, H.J.B., Lotter, A.F., Juggins, S., Smol, J.P. (Eds.), Tracking Environmental Change Using Lake Sediments, Developments in Paleoenvironmental Research 5, Developments in Paleoenvironmental Research. Springer Netherlands, Dordrecht, pp. 123–141. doi:10.1007/978-94-007-2745-8

Kanner, L.C., Burns, S.J., Cheng, H., Edwards, R.L., Vuille, M., 2013. High-resolution variability of the South American summer monsoon over the last seven millennia: insights from a speleothem record from the central Peruvian Andes. Quat. Sci. Rev. 75, 1–10. doi:10.1016/j.quascirev.2013.05.008

Leng, M.J., Marshall, J.D., 2004. Palaeoclimate interpretation of stable isotope data from lake sediment archives. Quat. Sci. Rev. 23, 811–831. doi:10.1016/j.quascirev.2003.06.012

Markgraf, V., 1989. Palaeoclimates in Central and South America since 18,000 BP based on Pollen and lake-level records. Quat. Sci. Rev. 8, 1–24.

Massaferro, J., Larocque, I.T., 2013. Using a newly developed chironomid transfer function for reconstructing mean annual air temperature at Lake Potrok Aike , Patagonia , Argentina. Ecol. Indic. 24, 201–210. doi:10.1016/j.ecolind.2012.06.017

Massaferro, J., Larocque-Tobler, I., Brooks, S.J., Vandergoes, M., Dieffenbacher-Krall, A., Moreno, P., 2014. Quantifying climate change in Huelmo mire (Chile, Northwestern Patagonia) during the Last Glacial Termination using a newly developed chironomid-based temperature model. Palaeogeogr. Palaeoclimatol. Palaeoecol. 399, 214–224. doi:10.1016/j.palaeo.2014.01.013

Matthews-Bird, F., Gosling, W.D., Coe, A.L., Bush, M., Mayle, F.E., Axford, Y., Brooks, S.J., 2015. Environmental controls on the distribution and diversity of lentic Chironomidae (Insecta : Diptera) across an altitudinal gradient in tropical South America. Ecol. Evol. 1–22. doi:10.1002/ece3.1833

Mayewski, P.A., Rohling, E.E., Curt Stager, J., Karlén, W., Maasch, K.A., David Meeker, L., Meyerson, E. a., Gasse, F., van Kreveld, S., Holmgren, K., Lee-Thorp, J., Rosqvist, G., Rack, F., Staubwasser, M., Schneider, R.R., Steig, E.J., 2004. Holocene climate variability. Quat. Res. 62, 243–255. doi:10.1016/j.yqres.2004.07.001

762 Meyer, I., Wagner, S., 2008. The Little Ice Age in southern Patagonia : Comparison between paleoecological
763 reconstructions and downscaled model output of a GCM simulation. PAGES news 16.

764 Mosblech, N. a. S., Bush, M.B., Gosling, W.D., Hodell, D., Thomas, L., van Calsteren, P., Correa-Metrio, A.,
765 Valencia, B.G., Curtis, J., van Woesik, R., 2012. North Atlantic forcing of Amazonian precipitation during the
766 last ice age. Nat. Geosci. 5, 817–820. doi:10.1038/ngeo1588

767 O'Brien, S.R., Mayewski, P. a., Meeker, L.D., Meese, D.A., Twickler, M.S., Whitlow, S.I., 1995. Complexity of
768 Holocene Climate as Reconstructed from a Greenland Ice Core. Science (80-.). 270, 1962–1964.

769 Olander, H., Korhola, a., Blom, T., Birks, H.J.B., 1999a. An expanded calibration model for inferring lakewater
770 and air temperatures from fossil chironomid assemblages in northern Fennoscandia. The Holocene 9, 279–
771 294. doi:10.1191/095968399677918040

772 Olander, H., Korhola, a., Blom, T., Birks, H.J.B., 1999b. An expanded calibration model for inferring lakewater
773 and air temperatures from fossil chironomid assemblages in northern Fennoscandia. The Holocene 9, 279–
774 294. doi:10.1191/095968399677918040

775 Oldfield, F., Steffen, W., 2014. Anthropogenic climate change and the nature of Earth System science. Anthr.
776 Rev. 1, 70–75. doi:10.1177/2053019613514862

777 Pinder, L.C.V., 1986. Biology of freshwater Chironomidae. Annu. Rev. Entomol. 31, 1–23.

778 Polissar, P.J., Abbott, M.B., Wolfe, a P., Bezada, M., Rull, V., Bradley, R.S., 2006. Solar modulation of Little Ice
779 Age climate in the tropical Andes. Proc. Natl. Acad. Sci. U. S. A. 103, 8937–42.
780 doi:10.1073/pnas.0603118103

781 Prat, N., Rieradevall, M., Acosta, R., Villamarín, C., M, G.D.I.F.E., 2011. Las Larvas de Chironomidae (Diptera) DE
782 Los rios Altoandinos de Ecuador y Peru, Clave par la determinacion de los generos.

783 Quinlan, R., Smol, J., 2001. Setting minimum head capsule abundance and taxa deletion criteria in chironomid-
784 based inference models. J. Paleolimnol. 26, 327–342.

785 Rees, A.B.H., Cwynar, L.C., Cranston, P.S., 2008. Midges (Chironomidae, Ceratopogonidae, Chaoboridae) as a
786 temperature proxy: a training set from Tasmania, Australia. J. Paleolimnol. doi:10.1007/s10933-008-9222-
787 6

788 Reuter, J., Stott, L., Khider, D., Sinha, A., Cheng, H., Edwards, R.L., 2009. A new perspective on the hydroclimate
789 variability in northern South America during the Little Ice Age. Geophys. Res. Lett. 36, L21706.
790 doi:10.1029/2009GL041051

791 Rieradevall, M., Brooks, S., 2001. An identification guide to subfossil Tanypodinae larvae (Insecta: Diptera:
792 Chrironomidae) based on cephalic setation. J. Paleolimnol. 81–99.

793 Self, A.E., Brooks, S.J., Birks, H.J.B., Nazarova, L., Porinchu, D., Odland, A., Yang, H., Jones, V.J., 2011. The
794 distribution and abundance of chironomids in high-latitude Eurasian lakes with respect to temperature
795 and continentality: development and application of new chironomid-based climate-inference models in
796 northern Russia. Quat. Sci. Rev. 30, 1122–1141. doi:10.1016/j.quascirev.2011.01.022

797 Telford, Birks, H.J.B., 2011a. A novel method for assessing the statistical significance of quantitative
798 reconstructions inferred from biotic assemblages. Quat. Sci. Rev. 30, 1272–1278.
799 doi:10.1016/j.quascirev.2011.03.002

800 Telford, Birks, H.J.B., 2011b. Effect of uneven sampling along an environmental gradient on transfer-function
801 performance. J. Paleolimnol. 46, 99–106. doi:10.1007/s10933-011-9523-z

802 Ter Braak, C.J.F., 1987. Ordination, in: Jongman, R.., ter Braak, C.J.., van Tongeren, O.F.R. (Eds.), Data Analysis in
803 Community Ecology. Pudoc, Wageningen, The Netherlands, pp. 91–173.

804 Ter Braak, C.J.F., Juggins, S., 1993. Weighted averaging partial least squares regression (WA-PLS): an improved
805 method for reconstructing environmental variables from species assemblages. Hydrobiologia 269/70, 485–
806 502.

807 Ter Braak, C.J.F., Looman, C.W.., 1986. Weighted averaging, logisitc regression and the Gaussian response
808 model. Vegetatio 65, 3–11.

809 Thompson, L.., Mosley-Thompson, E., Dansgaard, W., Grootes, P.., 1986. The Little Ice Age as Recorded in the
810 Stratigraphy of the Tropical Quelccaya Ice Cap. Science (80-.). 234, 361–364.

811 Thompson, L.G., Mosley-Thompson, E., Brecher, H., Davis, M., León, B., Les, D., Lin, P.-N., Mashiotta, T.,
812 Mountain, K., 2006. Abrupt tropical climate change: past and present. Proc. Natl. Acad. Sci. U. S. A. 103,
813 10536–43. doi:10.1073/pnas.0603900103

814 Thompson, L.G., Mosley-Thompson, E., Davis, M.E., 1995. Late glacial stage and Holocene tropical ice core
815 records from Huascaran, Peru. Science (80-.). 269, 46–50.

816 Thompson, L.G., Mosley-Thompson, E., Davis, M.E., Henderson, K.A., Brecher, H.H., Zagorodnov, V.S.,
817 Mashiotta, T.A., Lin, P.-N., Mikhalenko, V.N., Hardy, D.R., Beer, J., 2002. Kilimanjaro ice core records:
818 evidence of holocene climate change in tropical Africa. Science 298, 589–93. doi:10.1126/science.1073198

819 Thompson, L.G., Mosley-Thompson, E., Davis, M.E., Lin, P.N., Henderson, K.A., Cole-Dai, J., Bolzan, J.F., Liu, K.B.,
820 1995. Late glacial stage and holocene tropical ice core records from huascaran, peru. Science 269, 46–50.
821 doi:10.1126/science.269.5220.46

822 Trivinho-Strixino, S., 2011. Larvas de Chironomidae guia de Identificacao. Universidade Federale de Sao Carlos.

823 Van Geel, B., Raspopov, O.M., Renssen, H., Plicht, J. Van Der, Dergachev, V.A., Meijer, H.A.J., 1999. The role of
824 solar forcing upon climate change. Quat. Sci. Rev. 18, 331–338.

825 Velle, G., Brodersen, K.P., Birks, H.J.B., Willassen, E., 2010. Midges as quantitative temperature indicator
826 species: Lessons for palaeoecology. The Holocene 20, 989–1002. doi:10.1177/0959683610365933

827 Velle, G., Brooks, S.J., Birks, H.J.B., Willassen, E., 2005. Chironomids as a tool for inferring Holocene climate: an
828 assessment based on six sites in southern Scandinavia. Quat. Sci. Rev. 24, 1429–1462.
829 doi:10.1016/j.quascirev.2004.10.010

830 Vuille, M., Bradley, R., Keimig, F., 2000. Climate variability in the Andes of Ecuador and its relation to tropical
831 Pacific and Atlantic sea surface temperature anomalies. J. Clim. 13, 2520–2535.

832 Walker, I.R., Cwynar, L.C., 2006. Midges and palaeotemperature reconstruction—the North American
833 experience. Quat. Sci. Rev. 25, 1911–1925. doi:10.1016/j.quascirev.2006.01.014

834 Walker, I.R., Mathews, R.W., 1987. Chironomids, lake trophic status and climate. Quat. Res. 28, 431–437.

835 Wanner, H., Beer, J., Bütikofer, J., Crowley, T.J., Cubasch, U., Flückiger, J., Goosse, H., Grosjean, M., Joos, F.,
836 Kaplan, J.O., Küttel, M., Müller, S.A., Prentice, I.C., Solomina, O., Stocker, T.F., Tarasov, P., Wagner, M.,

Clim. Past Discuss., doi:10.5194/cp-2015-186, 2016
Manuscript under review for journal Clim. Past
Published: 20 January 2016

837 Widmann, M., 2008. Mid- to Late Holocene climate change: an overview. Quat. Sci. Rev. 27, 1791–1828.
838 doi:10.1016/j.quascirev.2008.06.013

839 Wiederholm, T., 1983. Chironomid of the Holarctic region. Keys and diagnosis. Part 1. Larvae. Entomologica
840 Scandinavica Supplement 19.

841 Woodward, C.., Shulmeister, J., 2006. New Zealand chironomids as proxies for human-induced and natural
842 environmental change: transfer functions for temperature and lake production (chlorophyll a). J.
843 Paleolimnol. 36, 407–429.

844 Wu, J., Porinchu, D.F., Horn, S.P., Haberyan, K. a., 2014. The modern distribution of chironomid sub-fossils
845 (Insecta: Diptera) in Costa Rica and the development of a regional chironomid-based temperature
846 inference model. Hydrobiologia 742, 107–127. doi:10.1007/s10750-014-1970-x

847

848

849

850

851 **Table captions**

852 **Table 1**

853 Summary of the physical and chemical properties of the 59 calibration data set lakes including the total number
854 of head capsules retrieved from each lake and the concentration of head capsules per gram of sediment. MAT=
855 mean annual temperature, MAP= mean annual precipitation, LOI=loss-on-ignition.

856 **Table 2**

857 Results of detrended canonical correspondence analysis (DCCA) using single constraining variables. MAT= mean
858 annual temperature, WT=water temperature, MAP=mean annual precipitation, LOI= Loss-on-ignition.

859 **Table 3**

860 Summary of the performance statistics of chironomid-based MAT inference models developed using classical
861 and Bayesian methods based on leave one out cross validation. Weighted averaging inverse and classical
862 (WAinv, WAcla), Weighted averaging partial least squares (WA-PLS), coefficient of determinant between
863 predicted and observed (r^2_{jack}), root mean squared error of prediction ($RMSEP_{jack}$) as % of the gradient.

864

Clim. Past Discuss., doi:10.5194/cp-2015-186, 2016
Manuscript under review for journal Clim. Past
Published: 20 January 2016

Climate of the Past Discussions
Open Access
EGU

865

866 **Tables**

867 **Table 1**

	Calibration data set				
	Minimum	Mean	Median	Maximum	Std dev
Conductivity (µs)	5.9	363	185	3205	579
Depth (m)	0.1	5	2.2	25	5.4
Elevation (m a.s.l)	150	3142	3845	4655	1459
Latitude (S)	0.1	11.2	14.2	17.3	6.2
Longitude (W)	64.4	71.6	70.3	78.4	4.5
LOI (%)	0	19	13	80	16
MAT (°C)	0.8	12	10	25	7
MAP (mm/year)	468	1222	769	4421	952
pH	5.7	8	7.9	10.2	1.1
Total Head Capsules	23	77	76	164	35
Water Temperature (°C)	5	15	13	33	6
Head capsule/gram	2	27	22	105	22

868

869 **Table 2**

870

Variable	Variance Explained (%)	λ_1/λ_2	*P*
MAT	12.93	1.431	0.001
MAP	10.3	0.900	0.001
WT	11.21	1.230	0.001
pH	6.23	0.500	0.001
LOI	3.23	0.239	0.062
Depth	2.44	0.190	0.240
Conductivity	2.34	0.179	0.296

871

872

873

874 **Table 3**

Model	R^2_{Jack}	$RMSEP_{jack}$	Mean $bias_{jack}$	Max $bias_{jack}$	% change
WA (inv)	0.890	2.404	-0.017	4.665	-
WA (cla)	0.890	2.475	-0.035	4.279	-2.936
WA-TOL (inv)	0.851	2.831	-0.182	6.498	-
WA-TOL (cla)	0.852	2.951	-0.211	7.350	-4.263
WA-PLS (1)	0.889	2.431	0.094	4.891	-
WA-PLS (2)	0.890	2.412	0.109	3.982	0.766
WA-PLS (3)	0.869	2.617	0.096	5.558	-8.483
WA-PLS (4)	0.866	2.659	0.199	5.922	-1.592
WA-PLS (5)	0.875	2.568	0.213	6.201	3.409
Bayesian	0.909	2.373	0.598	3.158	

875

876

Clim. Past Discuss., doi:10.5194/cp-2015-186, 2016
Manuscript under review for journal Clim. Past
Published: 20 January 2016

Climate of the Past Discussions
Open Access
EGU

877 **Figure captions**

878 **Figure 1**

879 Location of the calibration data set lakes (black circles) and Laguna Pindo (white triangle).

880 **Figure 2**

881 Figure 2: Canonical correspondence analysis (CCA) of the calibration data set lakes and environmental variables
882 with elevation and longitude removed after variance inflation analysis. MAP=mean annual precipitation,
883 MAT=mean annual temperature, WT= water temperature, LOI=loss-on-ignition. Grey circles denote calibration
884 lakes, dark grey triangles mark species. All species could not be labelled due to crowding; instead nine
885 important taxa have been marked as examples.

886 **Figure 3**

887 Chironomid taxa in the modern calibration dataset lakes. Lakes are ordered (top to bottom) from cold to warm
888 and chironomids are ordered by occurrence from cold to warm lakes. Only taxa present in three or more lakes
889 are included. Dashed line shows a gap in calibration data set lakes between 16-20 °C of the MAT gradient.
890 Detrended canonical correspondence analysis (DCCA) constrained by MAT shows the taxon turnover across the
891 gradient. Head capsule concentration (hc/gram) is also included.

892 **Figure 4**

893 Weighted-average and Bayesian optima (*solid grey circles*) and tolerances (*thick lines*) of the 55-chironomid taxa
894 included in the calibration dataset, MAT Range (*dashed lines*). Taxa are organised by WA temperature optima
895 from cold to warm.

896 **Figure 5**

897 Model performance of the best performing classical method (WA) and Bayesian approach. A=weighted
898 averaging method; B=Bayesian method. WA: R^2_{jack}= 0.890, $RMSEP_{jack}$ = 2.404, Mean $bias_{jack}$= -0.017, Max bias
899 $_{jack}$=4.665. Bayesian: R^2_{jack}= 0.909, $RMSEP_{jack}$ =2.373, Mean $bias_{jack}$= 0.598, Max $bias_{jack}$= 3.158.

900

Clim. Past Discuss., doi:10.5194/cp-2015-186, 2016
Manuscript under review for journal Clim. Past
Published: 20 January 2016

Figure 6

Diagram of fossil chironomid assemblage of Laguna Pindo. Five significant zones were identified using optimal partitioning with a broken stick model. Detrended canonical correspondence analysis (DCCA) constrained by calibrated radiocarbon age shows taxon turnover through time. Only taxa with relative abundances greater than 5% are shown. SD=standard deviation, hc/gram= head capsules per gram of wet sediment.

Figure 7

Chironomid-inferred mean annual temperatures (MAT) at Laguna Pindo using the WA inverse (grey) and Bayesian (black) models. Sample specific errors for the WA model are obtained through bootstrapping 999 cycles. Errors of the Bayesian reconstruction are site-specific uncertainties. Key late-Holocene climate events are shaded in grey. LIA=the range of the earliest and latest date for the Little Ice Age in South America (Polissar *et al*., 2006). 3500-2500 global cooling event (Mayewski *et al*., 2004), note, however, the Laguna Pindo record only extends to 3000 cal yrs BP.

Figure 8

Distribution of Laguna Pindo fossil samples (black circles) included passively within a CCA of the calibration data set lakes (grey circles) constrained using the significant environmental variables. MAP= mean annual precipitation, MAT= mean annual temperature, WT= water temperature. The first and last fossil sample in the sedimentary sequence has been labelled (total sediment depth); there are no directional trends through time. Calibration lakes that lie at similar elevations as Laguna Pindo have been labelled.

Figure 9

(left to right): Chironomid-inferred WA classical MAT with sample specific errors generated using bootstrapping. Bayesian reconstruction with sample specific errors. Goodness-of-fit of the fossil assemblages to temperature, vertical dotted line indicates the 90th percentile of squared residual distances of modern samples to first axis in a CCA; samples to the right of the line have a poor fit-to-temperature. Nearest modern analogue analysis,

Clim. Past Discuss., doi:10.5194/cp-2015-186, 2016
Manuscript under review for journal Clim. Past
Published: 20 January 2016

926 vertical dotted line indicates the 5th percentile of squared chord distances of the fossil samples in the modern
927 calibration data set; samples to the right of the line have no good modern analogues. Detrended canonical
928 correspondence analysis (DCCA) sample scores with radiocarbon age used as the sole constraining variable.
929 Head capsule concentration per gram of sediment. Zones are derived from optimal partitioning of fossil
930 assemblages using a broken stick model to define significant zones. Sq res dis= square residual distance; Sq chrd
931 dis= square chord distance; SD units= standard deviation units; hc/gram=head capsule per gram of sediment.

932 **Figure 10**

933 Histogram of the proportion of variance in the chironomid MAT transfer function explained by 999 transfer
934 functions trained on random environmental variables. Solid black line denotes the proportion of variance
935 explained by the chironomid WA inverse MAT transfer function. Black dashed line marks the proportion of
936 variance explained by the first axis of PCA of the fossil data. Grey dashed line marks the 95% variance of the
937 random reconstructions.

938 **Figure 11**

939 Individual likelihood functions for the fossil taxa in the coldest sample of the Laguna Pindo sequence (396 cm
940 total depth, *c.* 2700 cal yr BP). The posterior probability distribution for temperature for the fossil sample is
941 plotted in red, note this is plotted on an independent axis.

942

943

944

945

946

947

948

Clim. Past Discuss., doi:10.5194/cp-2015-186, 2016
Manuscript under review for journal Clim. Past
Published: 20 January 2016

Climate of the Past Discussions
Open Access
EGU

Figures

Figure 1

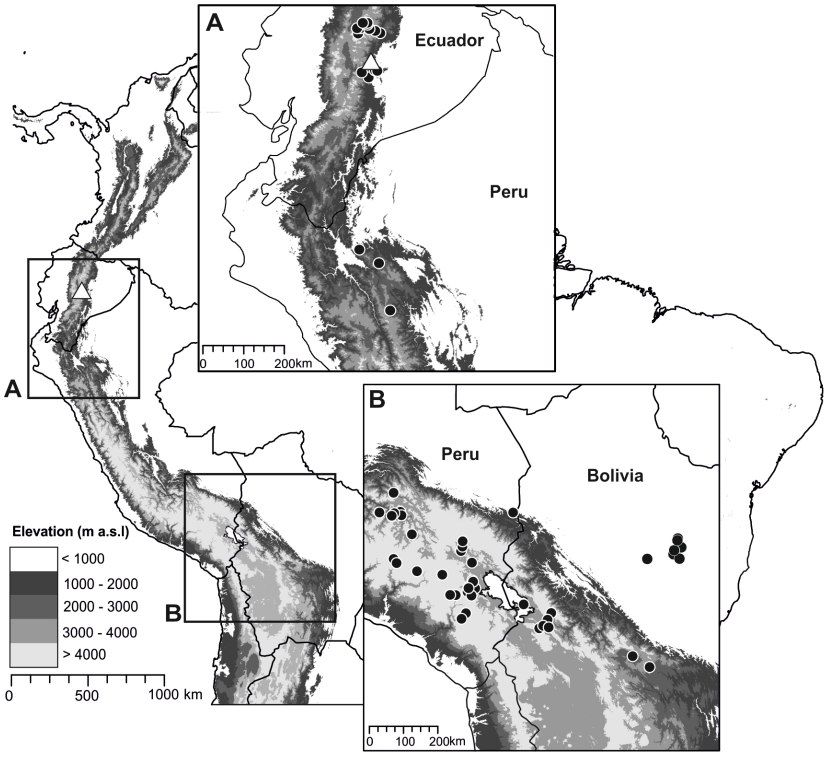

Clim. Past Discuss., doi:10.5194/cp-2015-186, 2016
Manuscript under review for journal Clim. Past
Published: 20 January 2016

Climate of the Past
Discussions
Open Access
EGU

974

975 **Figure 2**

976

977

978

979

980

981

982

983

984

985

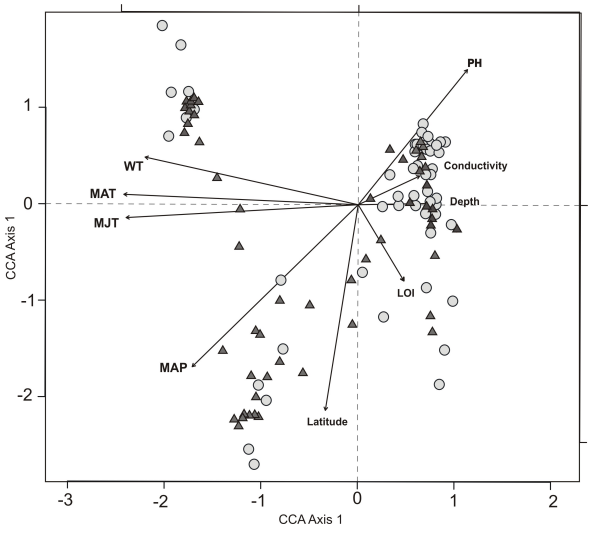

986

987

988

989

990

991

992

993

994

995

996

997

998

999

Clim. Past Discuss., doi:10.5194/cp-2015-186, 2016
Manuscript under review for journal Clim. Past
Published: 20 January 2016

Climate of the Past
Discussions
Open Access
EGU

Figure 3

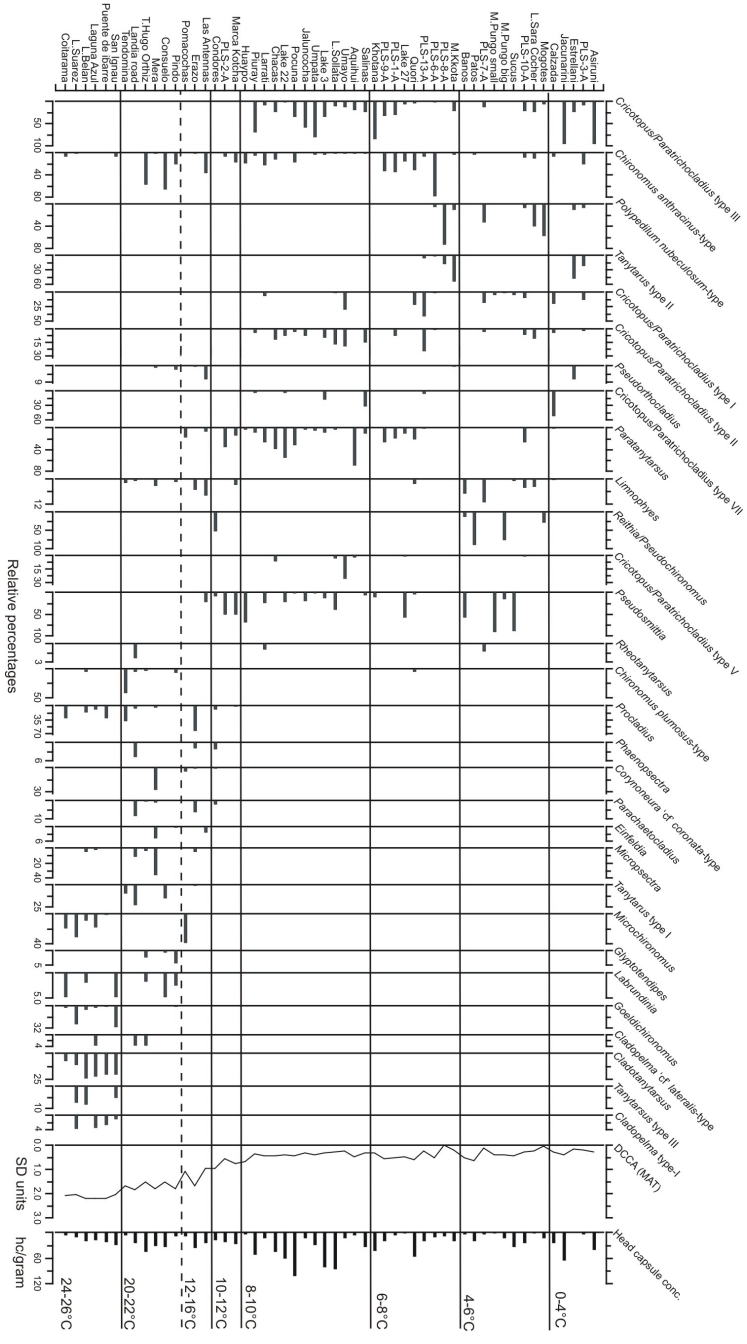

Clim. Past Discuss., doi:10.5194/cp-2015-186, 2016
Manuscript under review for journal Clim. Past
Published: 20 January 2016

Climate of the Past Discussions
Open Access
EGU

Figure 4

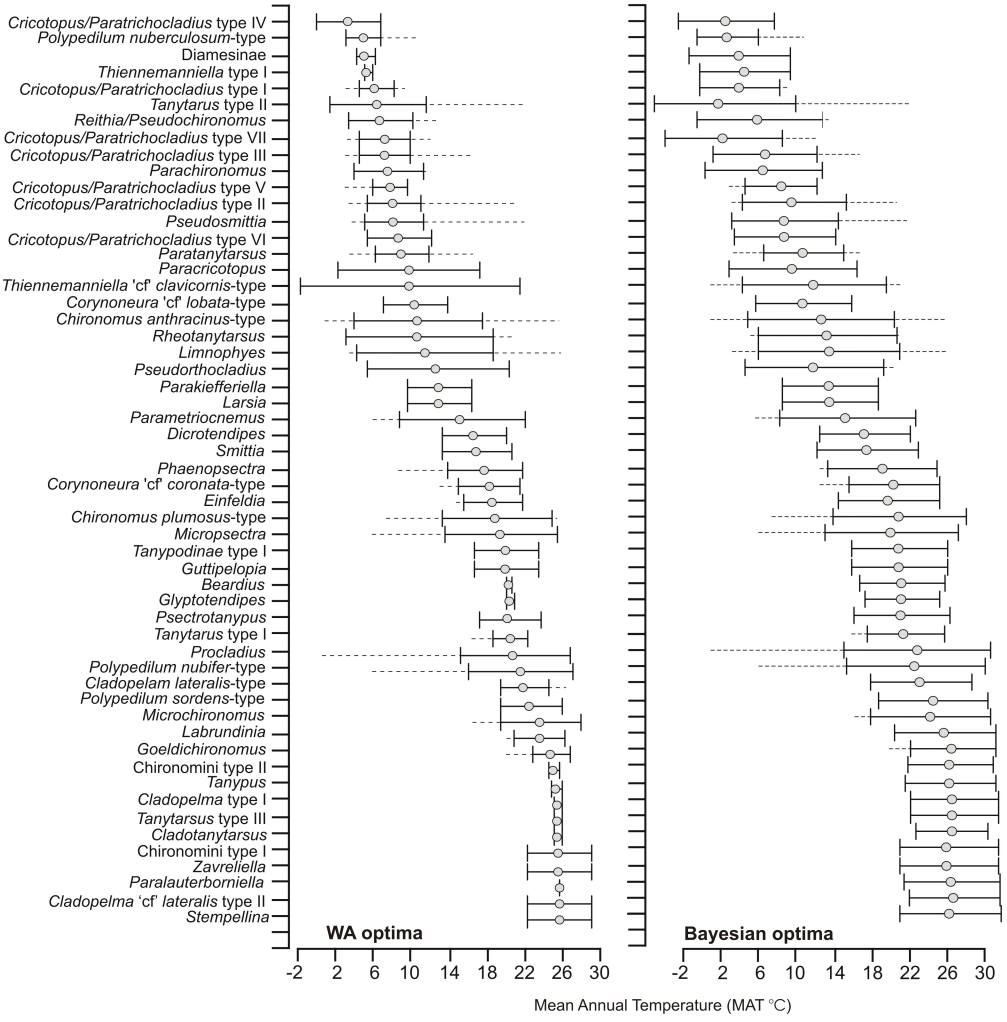

Clim. Past Discuss., doi:10.5194/cp-2015-186, 2016
Manuscript under review for journal Clim. Past
Published: 20 January 2016

Climate of the Past
Discussions
Open Access
EGU

052 **Figure 5**

053

054

055

056

057

058

059

060

061

062

063

064

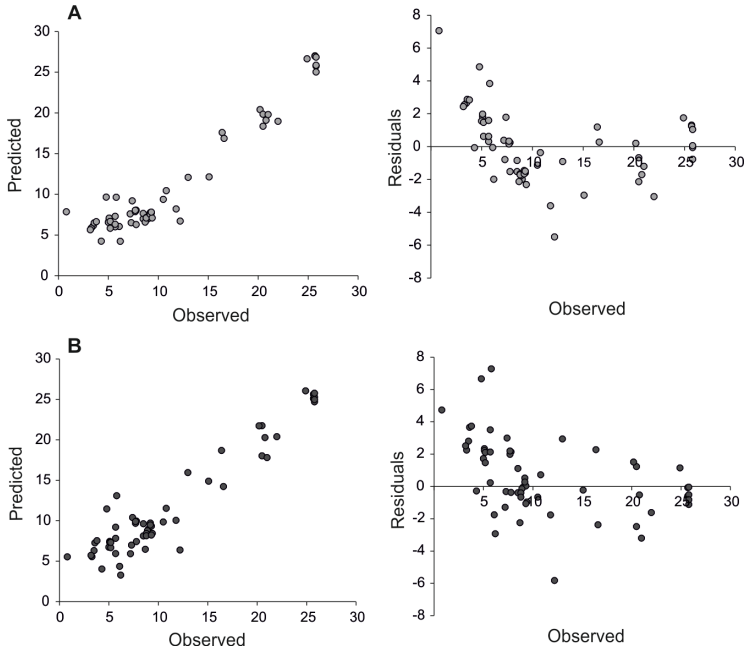

065

066

067

068

069

070

071

072

073

074

075

076

077

Clim. Past Discuss., doi:10.5194/cp-2015-186, 2016
Manuscript under review for journal Clim. Past
Published: 20 January 2016

Climate of the Past Discussions
Open Access
EGU

078 **Figure 6**

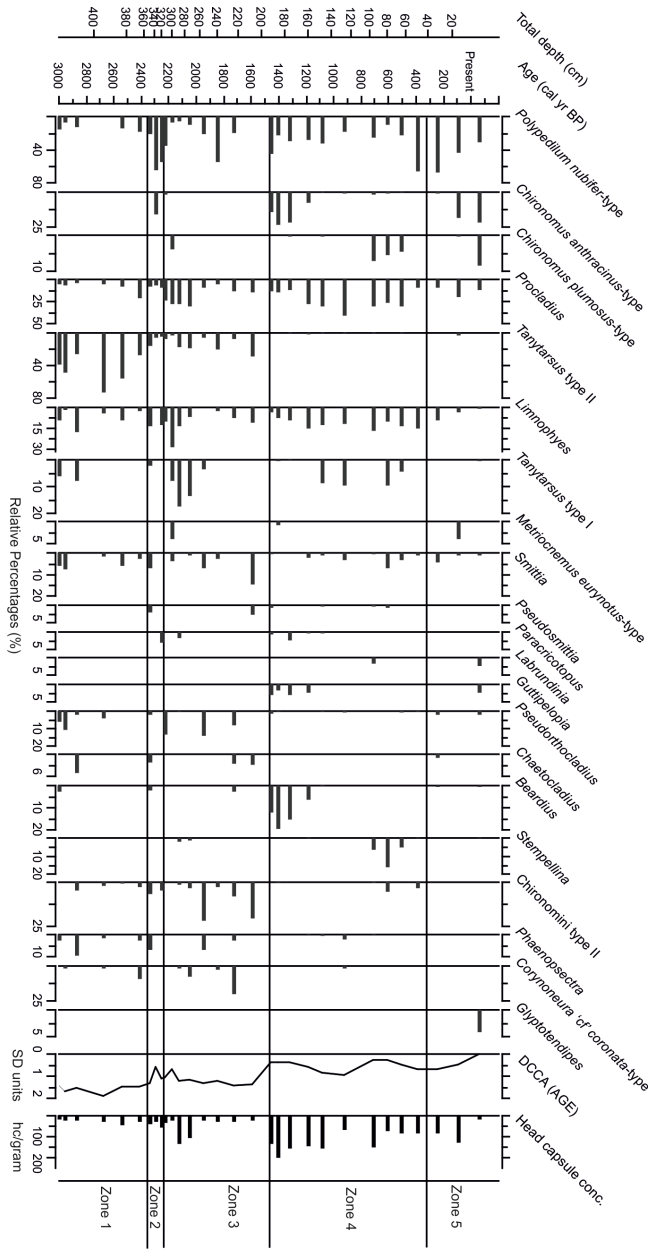

Clim. Past Discuss., doi:10.5194/cp-2015-186, 2016
Manuscript under review for journal Clim. Past
Published: 20 January 2016

Climate of the Past Discussions
Open Access
EGU

Figure 7

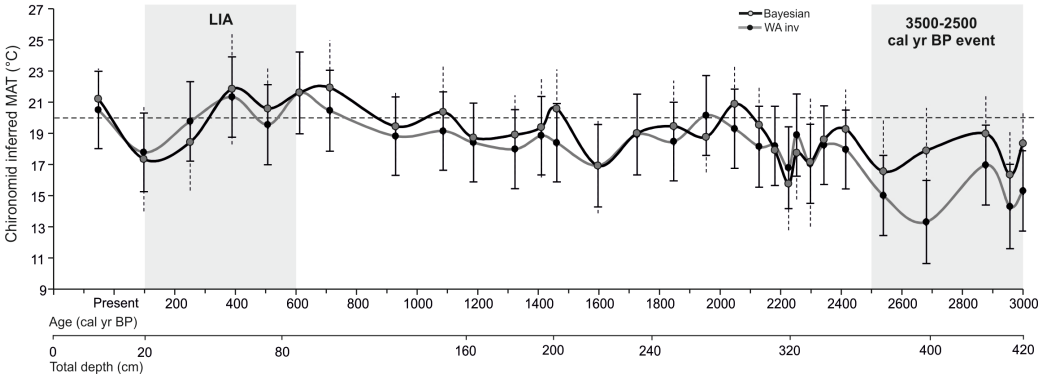

Clim. Past Discuss., doi:10.5194/cp-2015-186, 2016
Manuscript under review for journal Clim. Past
Published: 20 January 2016

Climate of the Past Discussions
Open Access
EGU

130 **Figure 8**

131

132

133

134

135

136

137

138

139

140

141

142

143

144

145

146

147

148

149

150

151

152

153

154

155

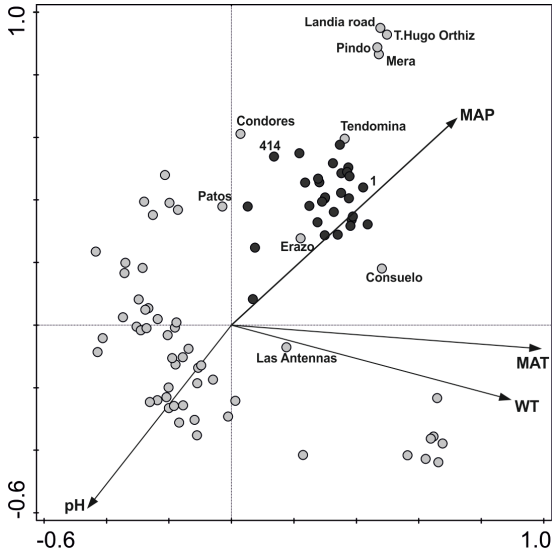

Clim. Past Discuss., doi:10.5194/cp-2015-186, 2016
Manuscript under review for journal Clim. Past
Published: 20 January 2016

Climate of the Past Discussions
Open Access
EGU

Figure 9

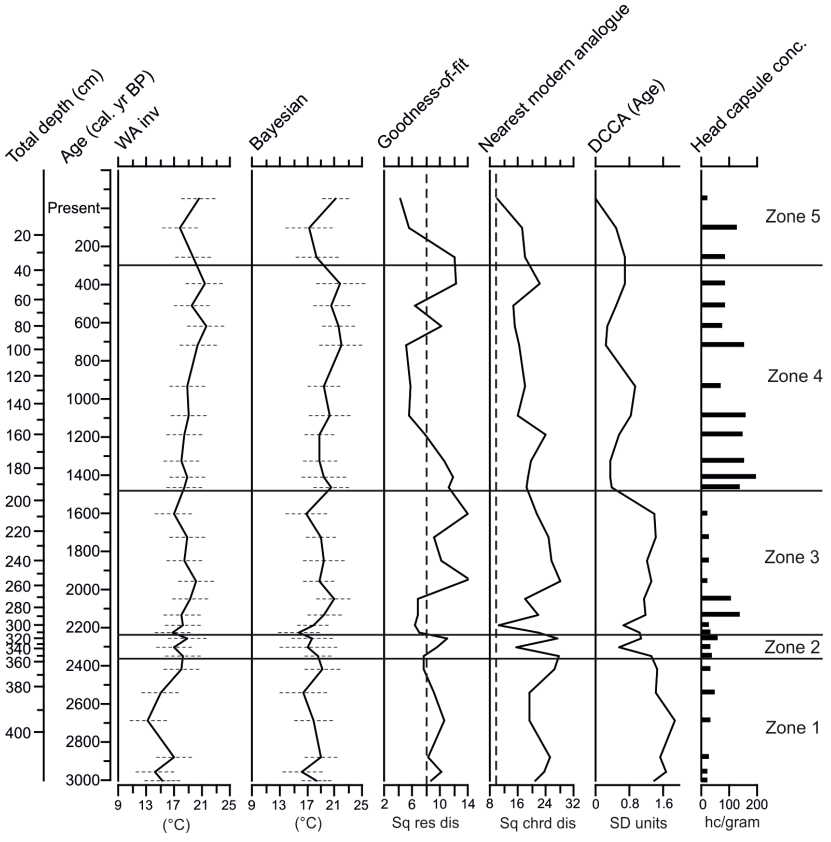

Clim. Past Discuss., doi:10.5194/cp-2015-186, 2016
Manuscript under review for journal Clim. Past
Published: 20 January 2016

Climate of the Past Discussions
Open Access
EGU

182

183 **Figure 10**

184

185

186

187

188

189

190

191

192

193

194

195

196

197

198

199

200

201

202

203

204

205

206

207

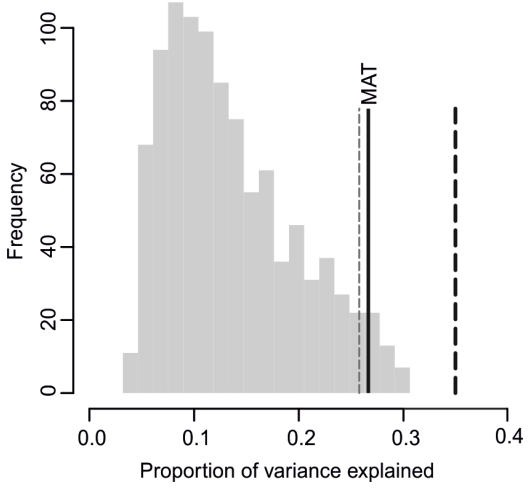

Clim. Past Discuss., doi:10.5194/cp-2015-186, 2016
Manuscript under review for journal Clim. Past
Published: 20 January 2016

Climate of the Past
Discussions
Open Access
EGU

208 **Figure 11**

209

210

211

212

213

214

215

216

217

218

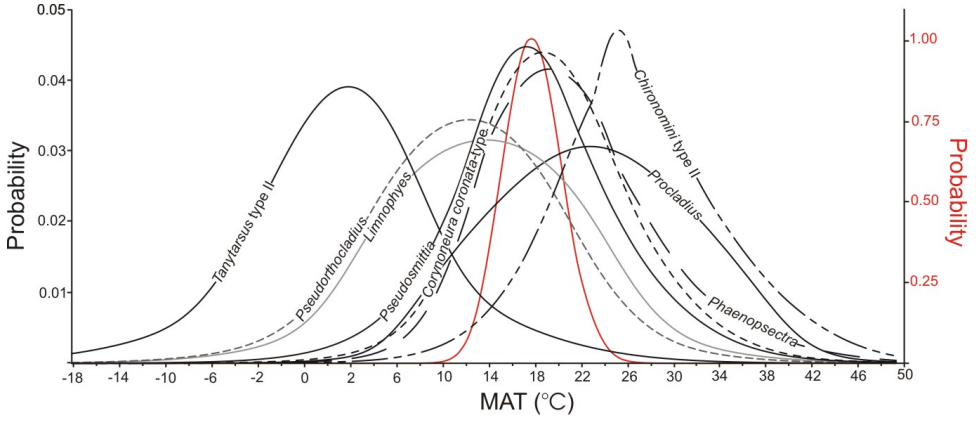

219

220

221

222

223

224

225

226

227

228

229